



HAL
open science

Practical Handbook of Grain Size Analysis Principles and methods

Jérôme Fournier-sowinski

► **To cite this version:**

Jérôme Fournier-sowinski. Practical Handbook of Grain Size Analysis Principles and methods. Station Marine. Zenodo, pp.75, 2024, 10.5281/zenodo.13836369 . hal-04703908

HAL Id: hal-04703908

<https://hal.science/hal-04703908v1>

Submitted on 20 Sep 2024

HAL is a multi-disciplinary open access archive for the deposit and dissemination of scientific research documents, whether they are published or not. The documents may come from teaching and research institutions in France or abroad, or from public or private research centers.

L'archive ouverte pluridisciplinaire **HAL**, est destinée au dépôt et à la diffusion de documents scientifiques de niveau recherche, publiés ou non, émanant des établissements d'enseignement et de recherche français ou étrangers, des laboratoires publics ou privés.



Distributed under a Creative Commons Attribution 4.0 International License

Practical Handbook of Grain-Size Analysis

Principles and methods



Jérôme Fournier-Sowinski



STATION MARINE
CONCARNEAU

Practical Handbook of Grain Size Analysis

Principles and methods

Jérôme Fournier-Sowinski

Centre National de la Recherche Scientifique

This practical handbook is designed for students who wish to perform particle size analysis using dry column sieving in accordance with current standards.

It is based on courses conducted at the Laboratoire de Géomorphologie et Environnement Littoral of the École Pratique des Hautes Études de Dinard. These courses include the Techniques d'Études en Géomorphologie Littorale, which was held annually until 2005, and the Master's course in Life and Earth Sciences, Environment, and Biodiversity Management. The author wishes to thank Pr. Fernand Verger† (ENS), Pr. Louis-Robert Lafon† (EPHE), Dr. Chantal Bonnot-Courtois† (CNRS), and Monique Le Vot (EPHE) for their role in establishing this course.

The main granulometric indices and descriptive statistics can be calculated with R using the G2Sd package developed by R. Gallon (INTECHMER) and J. Fournier-Sowinski (CNRS), available at the following address : <http://cran.r-project.org/web/packages/G2Sd/index.html>

This package has been described and published in:

Fournier J., Gallon R., Paris R., 2014. G2Sd: a new R package producing statistics on the distribution of unconsolidated sediments, *Géomorphologie, relief, processus, environnement* 14(1), p 73-78.

This document must be cited as follows:

Fournier-Sowinski J. 2024. *Practical Handbook of Grain Size Analysis. Principles and methods*. Marine Station MNHN, Concarneau, 75 p.

All photographs and figures are by the author, unless otherwise stated.

Chapter 1 Definitions

The purpose of granulometry is to measure the size of individual particles or grains. To ensure consistency and reliability, the measurement methods must be reproducible and adhere to strict standards. These methods include sieving, optical techniques, fluid sorting, and electrical methods.

- Dry sieving $> 40 \mu m$
- Wet sieving $> 30 \mu m$
- Sedimentometry 1 to $100 \mu m$
- Centrifugation 0.1 to $20 \mu m$
- Laser diffraction 10 nm to 3,5 mm
- Optical microscopy $> 20 \mu m$ to 2 mm

Granulometry also involves analyzing the statistical distribution of size classes within a collection of grains. Particle diameter is measured using the Feret diameter, which determines size in a specific direction. The exo-diameter is defined as the value of D where D_f is at its maximum, while the meso-diameter is defined as the value of D where D_f is at its minimum (Fig. 1).

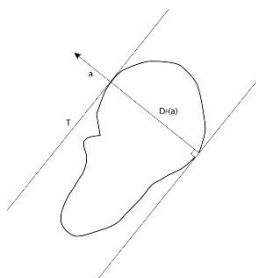


Fig. 1 Feret diameter

Grain shape can be characterized by an index that measures the surface area projected by the grain onto a circle with a diameter equal to the exo-diameter. The equivalent diameter refers to the diameter of a sphere that would exhibit the same behavior in a particle size analysis. It is important to note that a particle of bioclastic origin (with a shape resembling

a small plate or tile) will exhibit different sizes depending on the method used, such as laser diffraction granulometry or sieve column granulometry.

1.1 Dry and Wet Sieving Principles

Sieving involves measuring the weight of sediment retained by the meshes of calibrated sieves. The sieves are stacked in decreasing mesh size according to a mathematical progression. The weight of the sediment retained on each sieve (sieve reject) can then be determined. A sieve shaker is used to vibrate the entire stack of sieves for a specified period. This process can be performed dry for relatively coarse grains (such as silt). However, if the sediment consists of fine particles (such as mud), sieving is done under a flow of water or, less commonly, another liquid (such as alcohol). After sieving, each fraction is allowed to settle and dry before being weighed.

1.2 Sedimentometry Principle

This method involves measuring sedimentation time in a water column. Stokes' law, which describes the rate at which particles settle, is used to determine grain size. Several methods can be employed for this purpose.

- Andreasen pipette
- X-ray sedimentometry
- Martin's balance

The most common methods include the Andreasen pipette, which measures the concentration of material in the suspension at a specific height and

time, and X-ray sedimentometry, which assesses the absorption of radiation by the suspension at a given height and time, based on concentration. Additionally, the Martin balance measures the amount of material deposited on a tray over time.

1.3 Laser Diffraction Granulometry

Principle

Based on the principle of light diffraction, grains suspended in water diffract light emitted by a laser beam. The size of the particles alters the spatial distribution of the light, which is then recorded by photodiodes. The proportion of each size class is determined from this data. While this method is highly accurate, it is limited by the wavelength of the laser beam and the transparency of the grains. For accurate measurements, the grains must be sufficiently opaque and larger than the wavelength of the light. By considering the scattering and reflection of light by the grains, much smaller particle sizes can be measured, down to 10 nm. The latest laser diffraction granulometers utilize this principle, including models such as the Beckman Coulter LS 13 320 XR™, Malvern Mastersizer 3000+™, and Shimadzu SALD-2300™.

1.4 Image Analysis

Morphoscopic observations are conducted using a binocular loupe, and digital photographs are captured with a camera connected to a computer. These digital images can be analyzed using specialized software, such as ImageJ (<https://imagej.net/ij/>). This method allows for the measurement of grain sizes from a transformed (binary) image and can also be used to assess particle shape and determine its origin (morphoscopy and mineral nature). However, this

method has the inherent limitation of only providing measurements in two dimensions.

1.4.1 Grain Morphoscopy

Building on the pioneering work of Sorby (19th century) and Cayeux (1929), Cailleux developed morphoscopy, which involves sorting the granulometric fractions of a sediment sample and then classifying the grains by optical observation (magnification x5 to x80) based on shape and surface appearance. These characteristics reflect the grains' history and can offer insights into environmental evolution and sediment deposition modes. The goal of morphoscopy is to identify the environments in which grains were deposited.

Cailleux's Main Categories

- 1. Unworn grain:** They are characterized by an angular shape, regardless of whether the crystals are automorphic. The edges should show no signs of polishing or rounding. The surface can be either matte or shiny. These grains typically originate from granitic arenas and glacial deposits and are generally of proximal origin.
- 2. Rounded and shiny grain:** The edges of these grains are rounded to subspherical or spherical, and the surface is highly polished and shiny. These grains are typical of rivers, coastal beaches, and the continental shelf, indicating a more distal origin.
- 3. Rounded and dull grain:** The shape of these grains closely resembles a nearly perfect sphere. The surface is always frosted and matte. These grains are characteristic of aeolian transport and are commonly found in coastal dunes and sandy deserts.

1.4.2 Quartz Exoscopy

The surface of quartz grains is marked by numerous traces with shapes and sizes indicative of the factors that formed them. These factors may include physical, chemical, mechanical, or even biological origins.

Exoscopy allows for the observation and interpretation of these surface features through scanning electron microscopy, typically at magnifications between x50 and x5,000 (Fig. 2). Nearly 250 distinct features have been identified (Kransley & Doorkamp, 1973 ; Le Ribault, 1975, Mahaney, 2002). These features help determine a grain's depositional environment, its history, and sometimes its geographical origin. It is strongly recommended to focus on the 250-355 μm fraction. Samples are first washed in a bath of diluted hydrochloric acid (*HCl*), then rinsed with distilled

water. After drying, the grains are selected and metallized in a vacuum with gold, carbon, or silver.

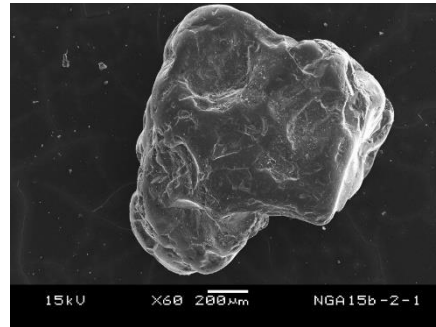


Fig. 2 SEM view of quartz grain, courtesy of R. Paris CNRS

1.5 Granulometric Definitions and Size

Classes

Granulometric definitions are numerous and vary depending on the authors, the spatial scale of the geographical areas studied, and the nature of the sediments encountered (Udden, 1914 ; Wentworth, 1922). Here are a few examples:

Bellair & Pomerol (1977)

Classes	Rudites	Angular blocks Rounded pebbles	20 mm
			Gravel
	Arenites	Sand	50 or 63 μm
		Fine sand	
Lutites	Silts	2 μm	
	Clays		

Bonnot-Courtois & Fournier-Sowinski (unpub.)

	Size	Denomination
2 mm	> 20 mm	Pebble (or Cobble)
	5 to 20 mm	Gravel
	2 to 5 mm	Granule
200 μm	1 to 2 mm	Coarse sand
	0.5 to 1 mm	Medium sand
	200 to 500 μm	Fine sand
63 μm	100 to 200 μm	Very fine sand
	63 to 100 μm	Coarse silt
	40 to 63 μm	Silt
	2 to 40 μm	Fine silt
	< 2 μm	Clay

Migniot (unpub.)

Rudites	Block Pebble Gravel	> 200 mm 20 to 200 mm > 2 to 20 mm
Arenites	Very coarse sand Coarse sand Medium sand Fine sand Very fine sand	1 to 2 mm 0.5 to 1 mm 0.25 to 0.5 mm 125 to 250 μm 63 to 125 μm
Lutites or Pelites	Silt Pre-colloids Colloids	4 to 63 μm 0.12 to 4 μm < 0.12 μm

Blair & McPherson, 1999 for gravels to boulders

Classe	Size (mm)
Sand	< 2
Gravel	2 – 4
Coarse gravel	4 – 8
Small pebble	8 – 16
Medium pebble	16 – 32
Large pebble	32 – 64
Small cobble	64 – 90
Medium cobble	90 – 128
Large cobble	128 – 180
Very large cobble	180 – 256
Small boulder	256 – 512
Medium boulder	512 – 1024
Large boulder	1024 – 2048
Very large boulder	2048 – 4096
Megaboulder	> 4096

Larsonneur (1977)

Type of sedimentary deposit	Characterization
Pebbles	> 50% of pebbles
Gravels	> 50% of pebbles and gravels
Sands	> 50% < 2 mm ; < 5% lutites
Gravel sand	> 15% of gravels
Coarse sand	Fraction 0.5 – 2 mm dominant
Fine sand	Fraction 0.2 – 0.5 mm dominant
Silts	Fraction 0.05 – 0.2 mm dominant
Muddy sediments	> 5% of lutites
Muddy sand	5% à 25% of lutites
Sandy mud	25% à 75% of lutites
Mud	> 75% of lutites

Udden (1914), Wentworth (1922), Friedman & Sanders (1978) and Blott & Pye (2001)

Particle size		Terminology			
ϕ	<i>mm/μm</i>	Udden (1914) Wentworth (1922)	Friedman & Sanders (1978)	Blott & Pye (2001)	
-11	2048 <i>mm</i>	Cobbles	Very large boulders	Very large Large Medium Small Very small	Boulders
-10	1024		Large boulders		
-9	512		Medium boulders		
-8	256		Small boulders		
-7	128		Large cobbles		
-6	64		Small cobbles		
-5	32	Pebbles	Very coarse pebbles	Very coarse Coarse Medium Fine Very fine	Gravel
-4	16		Coarse pebbles		
-3	8		Medium pebbles		
-2	4		Fine pebbles		
-1	2	Granules	Very fine pebbles		
0	1	Very coarse sand	Very coarse sand	Very coarse	Sand
1	500 <i>μm</i>	Coarse sand	Coarse sand	Coarse	
2	250	Medium sand	Medium sand	Medium	
3	125	Fine sand	Fine sand	Fine	
4	63	Very fine sand	Very fine sand	Very fine	
5	31	Silt	Very coarse silt	Very coarse Coarse Medium Fine Very fine	Silt
6	16		Coarse silt		
7	8		Medium silt		
8	4		Fine silt		
9	2	Clay	Very fine silt		
			Clay	Clay	

Chapter 2 Field Sampling

Sediment extraction in the field requires a variety of techniques, depending on factors such as the terrain, the specific problem, the type of analysis, the sediment type (ranging from silt to mega-boulders), and the quantity of sediment to be analyzed.

2.1 Particle Size Analysis

2.1.1 Indirect Access to Field

The nature of the terrain can vary significantly depending on its location—such as ocean, coastline, lake, pond, river, or inlet. The study site may be either directly or indirectly accessible. For work conducted at sea, in a river, or on a lake, sediment sampling often requires specialized equipment such as an oceanographic vessel, a semi-rigid boat, an underwater drone, a light kayak-type craft, or direct underwater diving.

Instruments for sediment extraction must be suited to the chosen vessel and include dedicated sediment grabs such as Shipeck, Eckman, Orange-Peel, Day, Ponar, Petersen, and Boxcorer, or benthos grabs that can also be used for sediment sampling, like Hamon, Smith-MacIntyre, and Van Veen (Fig. 3). When using a grab sampler, the sediment is mixed, which disrupts the original depositional structure. Additionally, it's important to remember that a grab sampler typically only captures the most recent sedimentary events, as it can only retrieve the top few centimeters or tens of centimeters of sediment.



Fig. 3 Smith Grab, N/O Louis Fage MNHN

When sampling with a grab sampler, the quantity of sediment collected is often considerable. Therefore, storage options and logistical issues, such as transport, must be carefully considered. Sediment is typically stored in large sample bags or watertight containers. For large-scale sampling campaigns, storage duration is also an important factor. For instance, if organic matter analysis is required, the sediment should be stored for a short period before analysis. Otherwise, the sediment can be frozen for longer-term storage. Granulometric analysis rarely covers the entire sample, so sub-sampling is necessary and must adhere to specific guidelines. In such cases, a sediment splitter is used.

2.1.2 Direct Access to Field

Field sampling is conducted directly for studies of dunes, beaches, sandbanks, pebble or boulder spits, and generally in the intertidal zone. Some operations may also be carried out underwater. Although the techniques used are similar to those on dry land, they need to be adapted to the specific conditions. The type of sediment will influence both the quantity of material to be collected and the method employed. For loose sediments, down to small gravels, a veterinary-type syringe can be used. This syringe, with a diameter smaller than that of a pillbox

(approximately 3 cm in diameter and 5 cm in height, giving a volume of about 141 cm³), is inserted into the sediment (Fig. 4). The contents are then transferred into the pillbox, which provides a volume ($\pi \times R^2 \times h$) sufficient for characterizing the sediment, either through sieving in a sieve column or by laser diffraction.



Fig. 4 Syringe and pillbox

When dealing with very coarse sedimentary material (such as gravel, pebbles, and boulders), the measurement technique changes significantly. Sampling such material for subsequent laboratory analysis can be challenging due to its weight and volume. Several methods have been developed for this type of material, including the Cailleux and Tricart methods (1959), or more recently, the Wolman method (Kondolf et al., 1993 ; Kondolf & Wolman, 1993). The Wolman method involves measuring the three axes of the pebbles (major axis *A*, intermediate axis *B*, and minor axis *C*) along a transect or within a quadrat.

The size of the sampling area must be carefully selected based on the size of the pebbles or blocks and their spatial distribution (e.g., regular, clustered, random, or spaced). Statistical tests can be valuable for planning before final data collection. Replication of samples is essential for statistical analysis. It is advisable to photograph the sampling area (preferably facing north) before measuring the pebbles with a caliper or similar tool. These photographs can later be used to analyze the

orientation of pebbles and boulders (Bellair & Pomerol, 1977 ; Chamley, 1988 ; Chamley & Deconinck, 2011).

Wolman Pebble Count

This technique involves measuring the sizes of random particles using a gravelometer. Particles smaller than 2 mm are categorized as <2 mm.

1. Select a Reach for Sediment Particle Size Distribution Quantification: For stream characterization, sample pools and riffles in proportion to their occurrence in the stream reach.

2. Start the Transect: Begin at a randomly selected point (e.g., by tossing a pebble) along the edge of the stream. Step perpendicularly into the water, and while avoiding looking directly, pick up the first pebble that touches your index finger next to your big toe.

3. Measure the b-Axis: Determine the pebble's size by identifying which hole it fits through in the gravelometer and record this measurement in your data book. For pebbles embedded in the sediment or those too large to move, measure the shortest visible axis.

4. Repeat Sampling: Take another step across the stream and repeat the process until you reach the opposite side. Establish a new transect and repeat the procedure. If the stream reach is relatively narrow (<2 m), you can modify the method by walking upstream in a zig-zag pattern rather than perpendicular to the flow. Collecting 100 measurements is generally considered an adequate sample size for accurately quantifying pebble distributions.

5. Data Analysis: After collecting the data, plot the sizes by class (using a log₂ scale) and frequency to determine the distributions. For instance, the D₅₀ value represents the particle size for which 50% of the samples are equal to or smaller.

2.2 Stratigraphic Analysis

Sediment sampling through core extraction allows for the analysis of deposit structures (e.g., sequence stratigraphy) and/or granulometric analyses, depending on the sediment's structure. Several types of equipment are available for core extraction, including hand-held corers, tube corers for long but narrow cores, and box corers (Reineck boxes) for short, wide samples.

In general, it is preferable to select a technique that preserves the integrity of the sediment. However,

sediment is often compacted, and edge effects may occur.

2.2.1 Hand-held Corer

Core sampling can be performed using PVC tubing, which is sealed at both ends once the sediment has been collected. The diameter of the tube is an important parameter and should be chosen based on the nature of the sediment in the study area (e.g., presence or absence of coarse elements that might limit depth). It is possible to manually extract cores several decimeters long (up to about 50 cm). Sometimes, it may be necessary to dig around the core to fully extract it from the sediment. This type of corer can be driven into the sediment by hand or with a sledgehammer, and it can also be used for underwater diving.

Hand auger drilling is still commonly used, primarily for reconnaissance purposes, though the sediments collected are often highly disturbed. Additionally, the Russian corer can be employed to extract 50 cm-long half-cores (PVC tubes split lengthwise) from easily penetrable sediments, such as peat bogs.

2.2.2 Reineck Box Corer

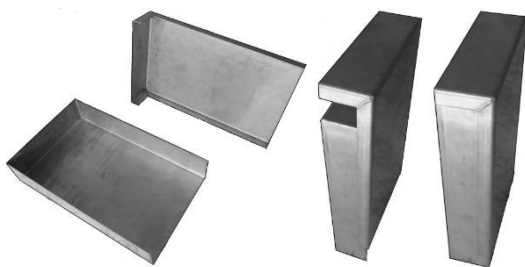


Fig. 5 Reineck box

The Reineck box consists of a bottomless square box, typically measuring 20-30 cm on each side and 50-80 cm in height (Fig. 5). A knife-edge plate along the box's sides cuts through the sediment, allowing for sample extraction. The design of the box can vary

in shape and size, depending on whether it is operated manually or with winches on oceanographic vessels.

The sediment-filled box is left to dry for three weeks in a dry, well-ventilated room. Once dry, the knife-edge plate is carefully removed. The sediment can then be stabilized with marine-grade resin. First, apply a layer of gauze over the sediment, followed by a second layer of resin. Allow the resin to dry for about a week. Afterward, the box can be turned upside down onto a sheet of marine plywood. Remove the box and let the sample dry for an additional week. Once the material is thoroughly dry, a small jet of water is used to wash away the unglued sediment, revealing the sedimentary structure, which can then be analyzed and interpreted.



Fig. 6 Results of a prepared sample

2.2.3 Tube and Multi-tube Corers

This corer consists of a long metal tube that sinks into the sediment by gravity. It features a removable liner and a sealing system similar to that of the Kullenberg corer. Multiple tubes can be arranged in a single frame (Fig. 7), allowing the corer to collect up to ten cores from a single location quickly, particularly in fine sand or mud environments. Various other corers are used in oceanography; for example, the N/O Marion Dufresne is equipped with a Calypso corer capable of extracting cores up to 60 meters long (Fig. 8).

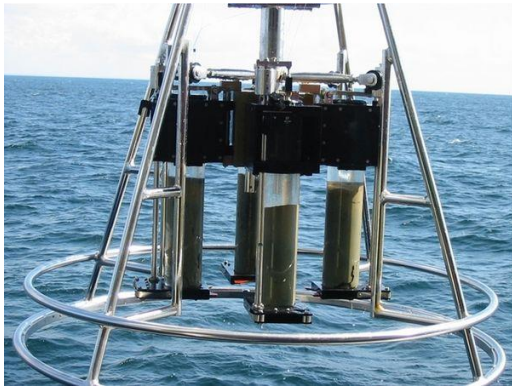


Fig. 7 Multi-tube corer, N/O Pourquoi Pas ? Ifremer



Fig. 8 Calypso corer, N/O Marion Dufresne TAAF/Ifremer

For terrestrial sampling, various types of motorized corers are employed, depending on the sediment or rock type to be penetrated and the required width and depth of the core. Below are two examples of motorized corers that facilitate drilling at greater depths and in terrains that are challenging to

penetrate with other methods (Figs. 9 and 10). Accurate control of drilling depth is essential, as compaction phenomena can occur.



Fig. 9 Motorized corer CNRS Caen



Fig. 10 Crawler-mounted motorized corer CNRS Clermont-

Ferrand

Chapter 3 Sieving Equipment

A sedimentology laboratory is equipped with various instruments and equipment for granulometric analysis (Fig. 11). Ideally, a designated work surface should be kept clear for washing and decanting samples. To give an idea of space requirements, 40 capsules with a 30 *cm* diameter placed side by side will cover an area of $\approx 3 \text{ m}^2$. The lab should also include dedicated workstations for tasks such as weighing, sample observation using a binocular magnifier and/or microscope, and possibly a computer station for data entry. The remaining space in the lab is used for drying, sieving, and chemical analysis.

Samples collected with a grab are generally stored in airtight plastic containers (Fig. 12). Sub-sampling is performed later in the laboratory.



Fig. 11 Lab equipped for granulometric analysis

3.1 Sampling and Storage

Various types of grabs are used to collect sediment, with the Shipek grab being one of the most commonly employed (Fig. 11). Its powerful spring mechanism ensures a nearly watertight seal, allowing it to retain fine sediments and function effectively on all types of seabeds, even those covered with pebbles and cobbles.



Fig. 11 Shipeck grab on ascent and opened with contents of maerl, N/O Côtes d'Aquitaine CNRS



Fig. 12 Airtight plastic container, N/O Côtes de la Manche CNRS

On the foreshore, in the dunes, the sediment sample can be collected using a veterinary syringe with a diameter smaller than that of the pillbox (Fig. 13) for coarse sediments ($< 5 \text{ mm}$). The sample name should be written with an indelible marker on both the side of the tube and the cap.



Fig. 13 Pillbox

3.2 Washing and cleaning

The contents of the pillbox are transferred into a capsule (Fig. 14), and distilled water is added. The sediment is then mixed with the water using a glass stirrer and allowed to settle until the water runs clear. The overflow is siphoned off using a surgical latex tube or similar. This process may be repeated several times until the sediment is completely desalted. During this procedure, tweezers should be used to remove any floating debris (such as algae or wood).

Some samples require more elaborate preparation. For instance, the sandy tubes produced by certain polychaete annelids present a challenge because the grains are bound together by biomineral cement. After rinsing the tubes, they are lightly etched with 50% hydrogen peroxide. The capsule is then placed on a hot plate at 40°C for about ten minutes. This causes the grains to gradually detach and settle at the bottom of the capsule. The internal mucosal tubes of the animal can be removed using forceps (Fig. 15).



Fig. 14 Porcelain capsule



Fig. 15 Decanted biogenic sediment (*Lanice conchilega* tube)

3.3 Drying

The decanted samples are placed in an oven (Fig. 16) for drying. Depending on the sediment type and the intended analysis, samples are dried for 24 to 48 hours at a temperature of 50°C to 60°C. A higher temperature should be avoided to prevent 'cooking' the sediment, especially in the case of clay-rich samples. Dried sediment may present a crust composed of fine baked sediments. This problem is often encountered. In this case, the crust must be very delicately broken down with a mortar and pestle. This is a delicate operation, as the risk is to create a finer sediment than the one initially present in the sample. To prevent this problem when the sediment is very rich in clay, the drying temperature should not exceed 30°C. The drying time is then adapted, sometimes up to 72 hours. While the oven is heating up, it is advisable to remain nearby to ensure it is functioning properly. Some ovens are

equipped with safety features, such as warning lights or alarms, to limit the temperature.



Fig. 16 Oven

3.4 Separating

The separator divides a sediment sample into two equal parts (Fig. 17), which is especially useful for samples collected using a shipboard grab. Since the volume of sediment is large, not all of it needs to be analyzed. The washed and dried sediment is poured into the separator's trough, where it is divided into two sub-samples, each collected in separate bins. This process is repeated until the desired volume of sediment is obtained.



Fig. 17 Jones precision riffle separator

Some analyses, such as calcimetry, require the sediment to be crushed using a mortar and pestle. This process inevitably compromises the integrity of the clasts, making any subsequent granulometric analysis highly biased.

3.5 Sieving

A sieve column (Fig. 18) consists of a stack of sieves, each with a progressively smaller mesh size, allowing for the separation of sediment by grain size. Typically, the finest sieves have a mesh size of 40 μm , while larger sieves, referred to as colanders, start at 3.315 mm. For reference, AFNOR sieves are graded as follows: 40, 50, 63, 80, 100, 125, 160, 200, 250, 315, 400, 500, 630, 800 μm , and 1, 1.25, 1.6, 2, 2.5 mm, with colanders at 3.315, 4, 5, 6.3, 8, 10, 12.5, 16, 20, and 25 mm. The sieve column is often placed in a sieve shaker, which vibrates the column to facilitate particle sorting. Other classifications, such as sieves measured in phi units, are also sometimes used.



Fig. 18 Sieve

The sieves are stacked in descending order, with the coarsest mesh at the top. The dry sediment is poured into the top of the column (Fig. 19), and a watertight base is used at the bottom to collect the fines.

The column is then placed on a sieve shaker (Fig. 19), which vibrates the sieves at a specified frequency for a set duration (typically 10 minutes). This process sorts the sediment by grain size. Each fraction is carefully poured into a capsule for weighing. Special attention should be given to removing any remaining grains from the sieve, using a brush suited to the fineness of the mesh. Brushes should never be used to press down on the sieve, and

grains trapped in the mesh should not be forcibly removed. Some cleaning systems use ultrasound.

It is essential that the sieves in the column remain matched and not interchanged. While it may be necessary to use a specific sieve size in the field, it should never come from a laboratory column. Sieve wear must be uniform, and for this reason, when replacing sieves, the entire column (or at least all the sieves) should be replaced together (LCPC, 1988).

3.6 Weighing

Each sieve fraction is weighed using a precision balance, which must be stabilized on a perfectly horizontal surface, tared, and protected from air movement (Fig. 20). It is also crucial that the precision balance is regularly calibrated by a certified organization. The measurements are recorded on paper and then entered into a spreadsheet for statistical analysis. The fractions are stored in clearly labeled bags for archiving. It is often useful to store fractions above and below 40 or 63 μm separately.



Fig. 19 Sieve column and sieve shaker



Fig. 20 Precision scale

3.7 Carbonizing



Fig. 21 Muffle furnace

The muffle furnace (Fig. 21) calcines the sediment at very high temperatures (up to 2000°C). Organic carbon C_{org} (produced by living organisms and bound to other elements such as H , N or P), inorganic

carbon C_{inorg} (associated with inorganic compounds, CO_2 ; $CaCO_3$) and carbonates can be measured indirectly, under certain conditions, using this type of furnace. The calcined sediment is then weighed once cooled in a desiccator. As a reminder, organic carbon is equal to the difference between total carbon and mineral carbon.

3.8 Calcium Carbonate

The Bernard calcimeter (Fig. 22) is used to measure the calcium carbonate content in sediment. The bioclastic material is first removed by etching with hydrochloric acid, and the $CaCO_3$ content is then measured indirectly. The calcimeter setup includes a bulb, a 100 cm^3 graduated tube, a 100 cm^3 Erlenmeyer flask, a small glass tube that is half the length of the Erlenmeyer flask, and two one-hole stoppers for the graduated tube and the Erlenmeyer flask. Due to the delicate nature of this procedure, it is essential to wear gloves, a cotton smock, and safety goggles.

Fig. 22 Bernard calcimeter



Chapter 4 Grain Size Analysis

4.1 Sample Treatment

4.1.1 Choice of Sediment Fraction to be Considered

Sediments can vary significantly in composition. Some are notably rich in calcium carbonate $CaCO_3$, which is typically of biogenic and/or phycogenic origin. The presence of shell fragments in the sediment can introduce complications, as large bioclasts may skew certain measurements.

In some cases, it may be preferable to analyze only the insoluble fraction of the sediment for particle size distribution. Systematically removing carbonate particles by pre-treating the sample with 10% hydrochloric acid (HCl) offers the following advantage:

- For the coarse fraction, it allows for analysis based on a particle stock with more uniform density (e.g., 2.65 for quartz sand).
- For the fine fraction, it aids in dispersing the sample. The Ca^{2+} and Mg^{2+} ions present in carbonates can cause colloid flocculation during analysis, as observed with coastal tange (carbonate-rich mud).

However, with certain precautions, it is possible to conduct particle size analysis without pre-treating the sample with hydrochloric acid. In this case, the sample is analyzed in its entirety.

4.1.2 Coarse fraction

It may be beneficial to consider the entire sediment sample, as bioclastic particles, like insoluble ones,

reflect key dynamic processes involved in transport and deposition (e.g., abrasion, particle size sorting). In some instances, the bioclastic fraction can account for over 95% of the total sediment (such as in shellfish beds, maerl beds, and *Crepidula fornicata* beds). However, the removal of carbonates is recommended to obtain accurate granulometric results in the following situations:

- When studying a sediment that was originally free of carbonates but has later been influenced by carbonate deposition.
- When analyzing a sediment in which carbonates have been recrystallized through diagenesis, altering their original particle size.

In such cases, it is necessary to remove the carbonates. However, for sediments like loess or tange, where carbonates may be a key component, it might be preferable to determine the granulometry of the total sediment, including carbonates. It's important to note that granulometric results can differ depending on whether carbonates are included or excluded.

Occasionally, whole shells or large, unworn bioclasts from species native to the studied environment (e.g., river, lake, or coastline) may be present. When this coarse material is not contemporaneous with the sediment's deposition, it distorts the natural grain size distribution. These large bioclasts should be removed before analysis.

Additionally, the density and especially the shape of bioclasts differ from the theoretical conditions needed to apply Stokes' law (which assumes spherical particles of constant density). This is

particularly true for particles larger than 0.2 mm. Even for the insoluble fraction, natural conditions often deviate from the ideal, due to the presence of heavy minerals (density > 3) or phyllosilicate minerals (such as biotite or muscovite), whose hydrodynamic behavior is very different from that of quartz particles.

4.1.3 Fine fraction (< 20 μm)

- The use of a laser diffraction granulometer offers the advantage of significantly reducing analysis time. This minimizes the risk of particle aggregation due to flocculation, which is a considerable concern in traditional free sedimentation measurements, such as those performed with Andreasen's short pipette, where the experiment can take up to 8 days.
- For particles of such small sizes, the settling rates of quartz and carbonate are nearly identical, and density variations within clay

minerals (kaolinite: 2.61; illite: 2.1–2.7; montmorillonite: 1.7–2.6) are far more significant.

4.1.4 Granulometric analysis diagram

The goal of granulometric analysis for unconsolidated sediments is to quantify the distribution of particle sizes within the sample.

While this process is straightforward for clean, homogeneous sands, it requires special preparation when samples contain a significant amount of fine material (silt and clay). The following documents outline the standard protocol used by the French Bureau de Recherche Géologique et Minière (BRGM) (Fig. 23), along with a sample data sheet (Tab. 1). This protocol can be adapted, modified, or simplified based on the specific research questions. It is provided here as an example. Data can be recorded in either AFNOR or ϕ format using the accompanying table (Tab. 2).

Tab. 1 Granulometric analysis data sheet

REF:						
Total weight:						
Analyzed weight						
AFNOR module	Sieve μm	Colander mm	Description	Weight g	%	Cumulative %
44		25				
43		20				
42		16				
41		12.5				
40		10				
39		8				
38		6.3				
37		5				
36		4				
35	2500	3.15				
34	2000					
33	1600					
32	1250					
31	1000					
30	800					
29	630					
28	500					
27	400					
26	315					
25	250					
24	200					
23	160					
22	125					
21	100					
20	80					
19	63					
18	50					
17	40					
	< 40					

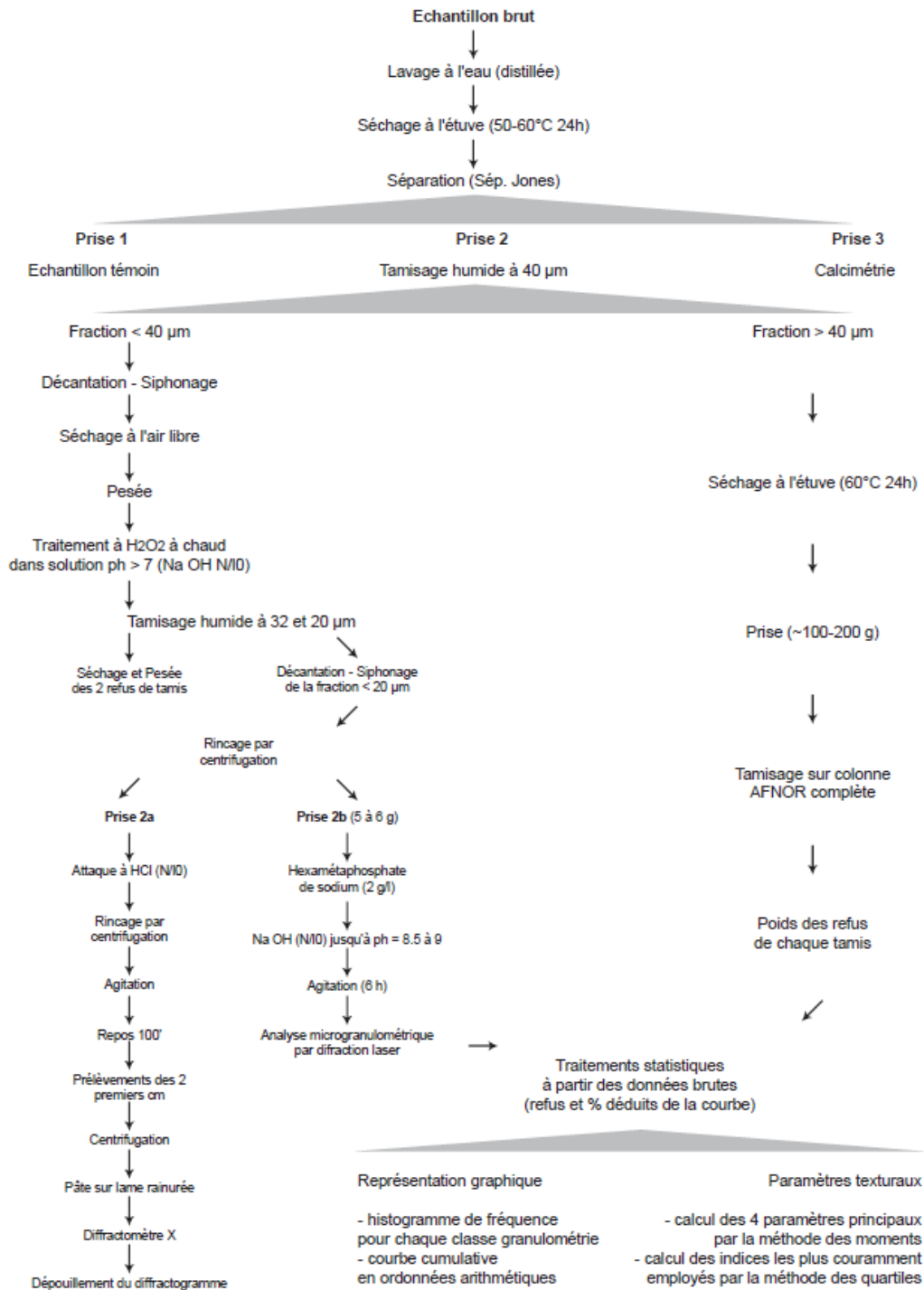


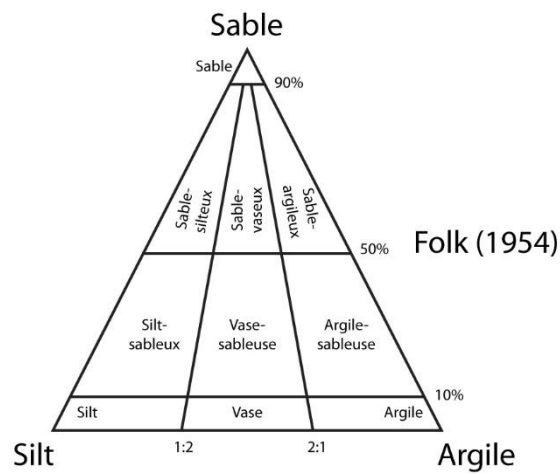
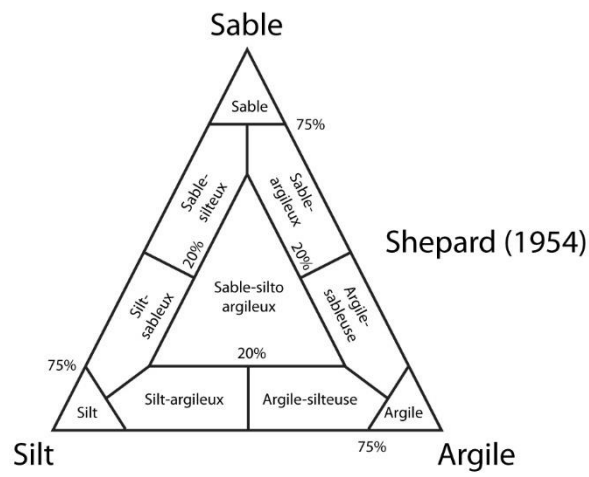
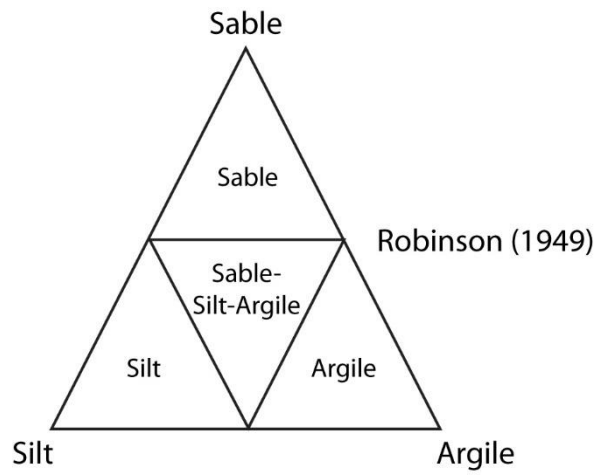
Fig. 23 Standard protocol used by the French BRGM (in French)

Tab. 2 Equivalence table between particle size units

AFNOR Module	<i>mm</i>	φ	Δ
38	5	-2.32	5.70
37	4	-2.00	5.60
36	3.15	-1.66	5.50
35	2.5	-1.32	5.40
34	2	-1.00	5.30
33	1.6	-0.68	5.20
32	1.25	-0.32	5.10
31	1	0	5.00
30	0.8	0.32	4.90
29	0.63	0.66	4.80
28	0.50	1.00	4.70
27	0.40	1.32	4.60
26	0.315	1.66	4.50
25	0.25	2.00	4.40
24	0.2	2.32	4.30
23	0.16	2.66	4.20
22	0.125	3.00	4.10
21	0.1	3.32	4.00
20	0.08	3.64	3.90
19	0.063	3.98	3.80
18	0.05	4.32	3.70
17	0.04	4.64	3.60
	0.0315	4.98	3.50
	0.025	5.32	3.40
	0.02	5.64	3.30
	0.016	5.96	3.20
	0.0125	6.32	3.10
	0.01	6.64	3.00
	0.008	6.96	2.90
	0.0063	7.30	2.80
	0.005	7.64	2.70
	0.004	7.96	2.60
	0.00315	8.30	2.50
	0.0025	8.64	2.40
	0.002	8.96	2.30
	0.0016	9.28	2.20
Lower limit	0.00063		0.86

$$\varphi = \log_2 \text{ the inverse of particle size in } mm : x_\varphi = -\log_2(x_{mm}) \rightarrow -3.32193 \log_{10}(x_{mm})$$

Fig. 24 Robinson, Shepard and Folk diagrams



4.1.5 Granulometric techniques

Samples submitted for particle size analysis can be processed using various methods, but it is important to note that the results will not always be directly comparable across methods.

- **Dry sieving:** This method uses AFNOR-type sieves for particle sizes ranging between $40\ \mu\text{m}$ and $25\ \mu\text{m}$. Sieving time is limited to 10 minutes to minimize the breakage of bioclasts, which are abundant in some samples. Certain sieve shakers offer continuous or intermittent vibration, with the choice depending on the sediment's nature (e.g., agglomerates that form after oven drying). In case of uncertainty, it is recommended to consult the sieve shaker's instruction manual.
- **Sieving underflow:** This is recommended for separating particles smaller than $40\ \mu\text{m}$ from coarser fractions or for refining the sub- $40\ \mu\text{m}$ fraction. Two sieves are typically used: one with a $32\ \mu\text{m}$ opening and another with a $20\ \mu\text{m}$ opening. This method helps reduce material heterogeneity and improves micro-granulometric analysis.
- **Laser diffraction:** This method is recommended for sediments with sub-spherical particles smaller than $2\ \text{mm}$, which are opaque and have uniform density. For further details, consult the user manuals provided by the laser diffraction granulometer manufacturers. However, this technique may not be suitable for all sediment types, particularly those with a high bioclastic content. It is possible to analyze one part of a sample to dry sieving and another part to laser diffraction, but in

such cases, the results should be interpreted separately (Beuselinck et al., 1998 ; Di Stefano et al., 2010 ; Dur et al., 2004 ; Konert & Vandenberghe, 1997 ; Ramswamy & Rao, 2006, Rodriguez & Uriarte, 2009). Nevertheless, for some sediments, the results from laser diffraction can be comparable to those obtained through sieving (Cheetham et al., 2008).

- **Sedimentometry using an X-ray sedigraph:** This method provides a granulometric curve for particles smaller than $20\ \mu\text{m}$, and potentially down to $2\ \mu\text{m}$, by measuring the rate at which particles settle by gravity in a liquid (typically water). The settling velocity is directly related to particle size, following Stokes' law:

$$V = C \cdot r^2 \text{ with } r = \left(\frac{V}{C}\right)^{\frac{1}{2}}$$
$$\text{with } C = \frac{2}{9} \cdot \frac{\rho - \rho_o}{\vartheta} \cdot g$$

with g Stokes constant ; r particle radius, ρ particle density, ϑ liquid viscosity, V particle fall velocity, ρ_o liquid density and g gravity acceleration.

Sedigraphs are commonly used to analyze clays. By utilizing a narrow X-ray beam, they measure the concentration of particles remaining in suspension at progressively lower sedimentation heights over time.

For very fine grains, particle shape plays a crucial role. Clay particles, for example, are plate-like rather than spherical. Static laser scattering granulometers rely on the interaction of light with particles, while dynamic scattering granulometers are based on Brownian motion and the viscosity of the mixture. Sediment samplers, on the other hand, operate based on hydraulic friction. These different methods interact with particles in various ways, resulting in

different particle size distributions. As a result, the measurements, particularly for clays, are often not directly comparable.

4.2 Data Processing

Graphical or digital processing of the raw sieving results is used to define the sample under study, using specific parameters (position, dispersion, asymmetry and kurtosis).

Most granulometric statistics can easily be calculated using R's G2Sd package, which has been described in Fournier J., Gallon R., Paris R., 2014. G2Sd: a new R package producing statistics on the distribution of unconsolidated sediments, *Geomorphology, relief, processes, environment* 14(1), p 73-78 and available at <http://cran.r-project.org/web/packages/G2Sd/index.html>

4.2.1 Percentile method

The cumulative curve reveals an initial set of parameters, from which all other values are derived. These are the Q_x percentiles, representing points corresponding to hypothetical sieve sizes, where $x\%$ of the sediment's weight consists of particles either larger or smaller than a given size. The most commonly used percentile values on the x-axis are 1, 5, 16, 25, 50, 75, 84, 95, and 99.

4.2.2 Position parameters

The **median**, or Q_{50} , is the most commonly used positional index, as it provides an estimate of the sediment's average grain size by encompassing all particle size classes.

The **mode** represents the particle size where the greatest accumulation, or maximum sieve residue," occurs on a sieve.

Quartiles Q_{25} and Q_{75} , along with percentiles Q_1 , Q_{16} , Q_{84} , Q_{95} , and Q_{99} , are rarely used in isolation (except for Q_{95} and Q_{99} in the Passega test). However, when combined, they form more complex indices.

4.2.3 Dispersion parameters

A sample's sorting can be determined by examining the slope of the cumulative curve or the spread of the frequency curve. Various indices can be used to quantify this sorting. The grading coefficients of sediments can indeed vary depending on the texture of the material. Fine and very fine sands tend to be better sorted (more uniformly graded) than medium and coarse sands at the same stage of evolution. This is because finer particles are more easily transported and deposited under uniform energy conditions, which allows them to settle in a more sorted manner.

In contrast, medium and coarse sands are usually subject to more variable energy conditions during transport and deposition. These larger particles are typically moved by higher energy processes, such as strong currents or waves, which can fluctuate in intensity. As a result, medium and coarse sands often exhibit poorer sorting, with a wider range of grain sizes present. This variability in sorting and grading reflects the dynamic nature of sedimentary environments and the energy conditions that influence the distribution and deposition of different sediment textures.

The **Trask Sorting Index So** is a measure of the degree of sorting of sediment grains. It is used to quantify how well or poorly sorted a sediment sample is. The index is calculated using the grain size distribution, typically based on the quartile values of the grain size. The formula for the Trask Sorting Index is:

$$So_{(mm)} = \sqrt{\frac{Q_{75}(mm)}{Q_{25}(mm)}}$$

Where: Q_{75} is the grain size at the 75th percentile (the upper quartile), Q_{25} is the grain size at the 25th percentile (the lower quartile).

The interpretation of the So value is as follows:

$So \approx 1$: Indicates a perfectly homogeneous sediment sample, meaning the grains are well-sorted and have similar sizes.

$So > 1$: Indicates increasing heterogeneity, meaning the grains are poorly sorted and there is a wide range of grain sizes present in the sample.

As So increases, the sediment becomes more heterogeneous, indicating a wider distribution of particle sizes.

So	Sorting
1 to 1.17	Very well sorted
1.17 to 1.20	Well sorted
1.20 to 1.35	Fairly well sorted
1.35 to 1.87	Moderately sorted
1.87 to 2.75	Poorly sorted
> 2.75	Very poorly sorted

The Krumbein Index $Q_{d\phi}$. Quartiles are expressed in ϕ units.

$$Q_{d\phi} = \left(\frac{Q_{d25} - Q_{d75}}{2} \right)$$

The relationship between heterometry and the parameter $Q_{d\phi}$ can be described using the concept that $Q_{d\phi}$ measures the degree of size variation in a sediment sample. When $Q_{d\phi} = 0$, it indicates perfect classification, meaning all particles are of the same size (no heterometry). As $Q_{d\phi}$ increases, it indicates

greater size variation among particles, hence increasing heterometry. Mathematically, this relationship can be expressed as:

$Q_{d\phi} = 0$ implies perfect classification (no heterometry).

$Q_{d\phi} > 0$ implies increasing heterometry.

This implies a direct proportional relationship between $Q_{d\phi}$ and heterometry, where heterometry is essentially a function of $Q_{d\phi}$. The mathematical relationship between these two parameters is :

$$Q_{d\phi} = \log_{10} \cdot So$$

The Folk & Ward dispersion Index $D_{FW\phi}$. The

Folk & Ward Dispersion Index is a parameter used in sedimentology to describe the spread or sorting of grain sizes in a sediment sample. Unlike other indices that focus on central measures such as mean, median, or mode, this index uses the tails or ends of the cumulative grain size distribution curve to determine the sorting characteristics. It provides a measure of how well or poorly the grains are sorted by considering both the finest and coarsest fractions of the sediment. To calculate the Folk & Ward Dispersion Index, you typically need to determine the grain sizes at specified percentiles (usually at the 5th, 16th, 50th, 84th, and 95th percentiles) on the cumulative frequency curve. The index helps in understanding the energy conditions during sediment transport and deposition, as well-sorted sediments usually indicate more uniform energy conditions, while poorly sorted sediments suggest fluctuating energy environments.

$$D_{FW\phi} = \frac{Q_{84\phi} - Q_{16\phi}}{4} + \frac{Q_{95\phi} - Q_{5\phi}}{6.6}$$

The Otto & Inman dispersion Index D .

$$D = \frac{Q_{84\phi} + Q_{16\phi}}{2}$$

The McCammon dispersion Index D .

$$D = 5.4 [(\phi_{85} - \phi_{15}) + (\phi_{95} - \phi_5)]$$

The Cailleux dispersion Index H_e . It is defined by the inter-quartile range showing the steepest slope for the cumulative curve. Low values indicate weak heterometry.

$$H_e = Q_{50} - Q_{75} \text{ ou } H_e = Q_{25} - Q_{50}$$

The Pomerol heterometry Index H_q . Expressed in α ($\alpha = 3\phi$), it is defined as:

$$H_q = \frac{Q_{25\alpha} - Q_{75\alpha}}{2}$$

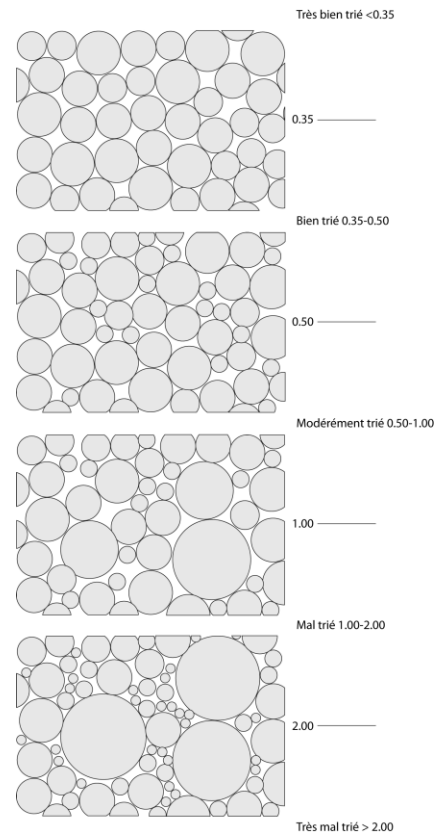
It is very close to the Krumbein index since $H_q = 3Q_{\alpha\phi}$.

Folk & Ward's medium grain M_G . Folk and Ward's method for analyzing sediment grain size includes calculating the median grain size, which is a measure of the central tendency of the grain size distribution. The median grain size is the diameter at which 50% of the sample's grain size distribution is finer, and 50% is coarser. It provides an indication of

the most common particle size within a sediment sample. The median grain size is often used in conjunction with other parameters like sorting, skewness, and kurtosis to provide a more comprehensive understanding of sediment characteristics and the processes that influenced their deposition.

$$M_G = \exp \frac{\ln P_{16} + \ln P_{50} + \ln P_{84}}{3}$$

Fig. 25 Visual standard for estimating Folk & Ward sorting (modified from Folk & Ward, 1957)



4.2.4 Asymmetry parameters

In addition to position and dispersion parameters, asymmetry parameters are essential for accurately defining a particle size distribution curve. These parameters measure the shape of the distribution on either side of the median, providing insight into the

The Krumbein asymmetry Index, expressed in Φ :

$$SK_{\sigma} = \frac{Q_{25\phi} + Q_{75\phi} - 2Q_{50\phi}}{2}$$

On the frequency histogram, three possible scenarios can occur depending on the values of this index.

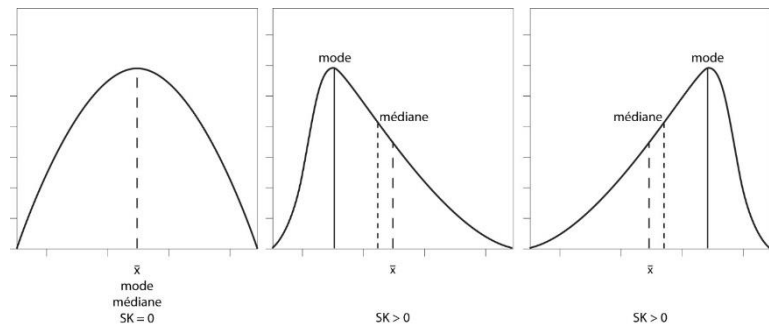


Fig. 26 Asymmetry index and frequency curve shape

skewness of the grain size distribution. Several indices have been proposed to quantify this asymmetry, each offering a different perspective on how the distribution deviates from symmetry around the median.

The Trask asymmetry Index:

$$ast = \frac{Q_{25(mm)} \times Q_{75(mm)}}{Q_{50(mm)}^2}$$

The Inman asymmetry Index (central part). Negative values indicate a dominance of fine sediments, whereas positive values suggest a prevalence of coarse sediments.

$$a\phi = \frac{\phi_{16} + \phi_{84} - 2\phi_{50}}{\phi_{84} - \phi_{16}}$$

The Inman asymmetry Index (extremities):

$$a(2\phi) = \frac{\phi_5 + \phi_{84.95} - 2\phi_{50}}{\phi_{84} - \phi_{16}}$$

1. $SK = 0$ (ou $ast = 1$), the mode coincides with the median and the mean, fine and coarse fractions are classified symmetrically with respect to the median,
2. $SK > 0$ (ou $ast < 1$), the coarse fraction is larger and therefore better classified than the fine fraction. The median and mode are to the left of the mean,
3. $SK < 0$ (ou $ast > 1$), the fine fraction is ranked higher than the coarse fraction. The median and mode are this time to the right of the mean.

The intermediate value of 0.3 is often used for skewness. For example, $-0.1 < SK < -0.3$ finely skewed or $-0.1 < SK < -0.3$ very finely skewed. SK between -0.1 and 0.1 characterize symmetrical distributions.

The Pomerol asymmetry Index, identical to the previous index, it is only expressed in α units. We find the equivalence $A_{sq\alpha} = 3SK_{\phi}$

$$A_{sq\alpha} = \frac{Q_{75\alpha} + Q_{25\alpha} - 2Q_{50\alpha}}{2}$$

4.2.5 Sharpness parameters

The Inman sharpness Index (or Kurtosis):

$$K = \frac{(Q_{95\alpha} - Q_{5\alpha}) - \phi}{\sigma_{\phi}}$$

σ_{ϕ} = standard deviation in units ϕ . The value of K varies around 1 ; thus if $0.90 < K < 1.11$, the curve is said to be mesokurtik; it is platykurtic if $0.67 < K < 0.90$ and leptokurtic if $1.11 < K < 1.50$.

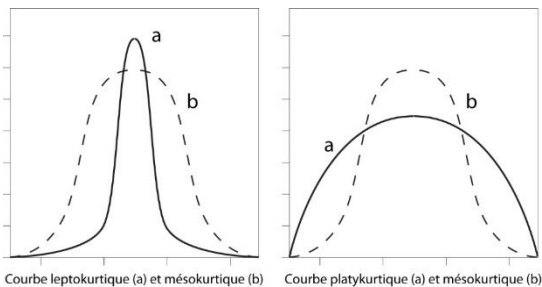


Fig. 27 Acuity parameters and frequency curve shape

The Krumbein & Pettijohn sharpness Index (or Kurtosis):

$$K = \frac{Q_{75(mm)} - Q_{25(mm)}}{2(Q_{90(mm)} - Q_{10(mm)})}$$

The Folk & Ward sharpness Index (or Kurtosis):

$$K_g = \frac{Q_{95\phi} - Q_{5\phi}}{2.44(Q_{75\phi} - Q_{25\phi})}$$

4.3 Graphical Representation

This description refers to a common method for analyzing grain and particle size distributions, particularly in sedimentology and soil mechanics.

- **X-Axis (Abscissa):** The particle sizes corresponding to the mesh openings of AFNOR-type sieves are plotted on a logarithmic scale.
- **Y-Axis (Ordinate):** The cumulative percentages of particles larger than the size given on the x-axis are plotted on an arithmetic scale.
- **Cumulative Curve:** This curve shows the percentage of the total sample weight that is retained by or passes through each sieve. It typically starts at 100% for the smallest size and decreases as particle size increases.

This representation allows for a quick visual assessment of the sediment's grain size distribution and is a standard method in sedimentology. It provides insights into the sediment's depositional environment and can be used to infer various physical properties.

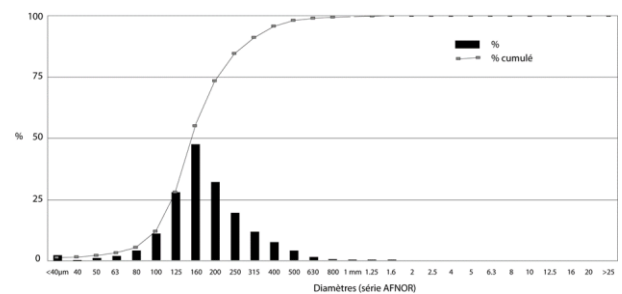


Fig. 27 Classical representation of a particle size analysis

The \emptyset scale is a logarithmic scale frequently used by Anglo-Saxon authors to express particle sizes, particularly in sedimentology and geology. Parameters like mean, sorting, skewness, and kurtosis can be easily calculated using this scale. This scale simplifies the representation and analysis of particle size distributions by transforming the sizes into a linear scale, making it easier to handle the wide range of sediment sizes. The \emptyset scale is defined as the negative base-2 logarithm of the particle diameter in millimeters:

$$x_{\emptyset} = -\log_2(x_{mm})$$

- Alternatively, using the change of base formula for logarithms:

$$x_{\emptyset} = -3.32193 \log_{10}(x_{mm})$$

The scale is arbitrarily set so that a particle diameter of 1 mm corresponds to:

$$x_{mm} = 1 \Rightarrow x_{\emptyset} = -\log_2(1) = 0$$

Each unit change in \emptyset represents a doubling or halving of particle size. For example:

$$x_{\emptyset} = 1 \Rightarrow x_{mm} = 0.5 \text{ mm}$$

$$x_{\emptyset} = -1 \Rightarrow x_{mm} = 2 \text{ mm}$$

The relationship between particle diameter in *mm* and \emptyset is exponential. Negative \emptyset values indicate particles larger than 1 *mm*, while positive \emptyset values indicate particles smaller than 1 *mm*. For example:

$$x_{mm} = 2^{-x_{\emptyset}}$$

$$x_{\emptyset} = 2^{-2} = 0.25 \text{ mm}$$

$$x_{\emptyset} = 2^{-(-3)} = 2^3 = 8 \text{ mm}$$

4.3.1 Evolution index method

The Rivière method, known for its precision and originality, requires a specific logarithmic scale on the abscissa axis. The recommended scale is either a base-10 logarithmic scale or a Δ scale. Additionally, with the dimensional unit set at 1/100 of a micrometer (μm), we have:

$$\begin{aligned} X\Delta &= \log_{10} \times x_{mm} = \log_{10} 10^5 \mu\text{m} \times 10^{-2} \\ &= 5 \end{aligned}$$

Cumulative weight percentages are represented as ordinates on an arithmetic scale. When the sample analyzed for particle size contains a significant fraction (over 10%) of lutite (with a diameter less than 50 μm , additional methods can be employed. Alongside sieving for arenites (ranging from 50 μm to 2 *mm*) and rudites (greater than 2 *mm*) a sedigraph or laser diffraction granulometer can be used to determine the particle size distribution of this fine fraction (less than 20 μm).

However, the analysis of this fraction (which can also be conducted using Andreasen's short pipette) provides information on the equivalent dimensions of the particles in suspension, determined by their falling velocity. These equivalent dimensions are not the actual particle sizes; rather, they correspond to the diameter of spherical quartz particles with the same falling velocity. Therefore, they do not reflect the real dimensions of the particles. The curve plotted by the sedigraph or laser diffraction granulometer is directly expressed in equivalent dimensions, applying Stokes' formula to the terminal fall velocity.

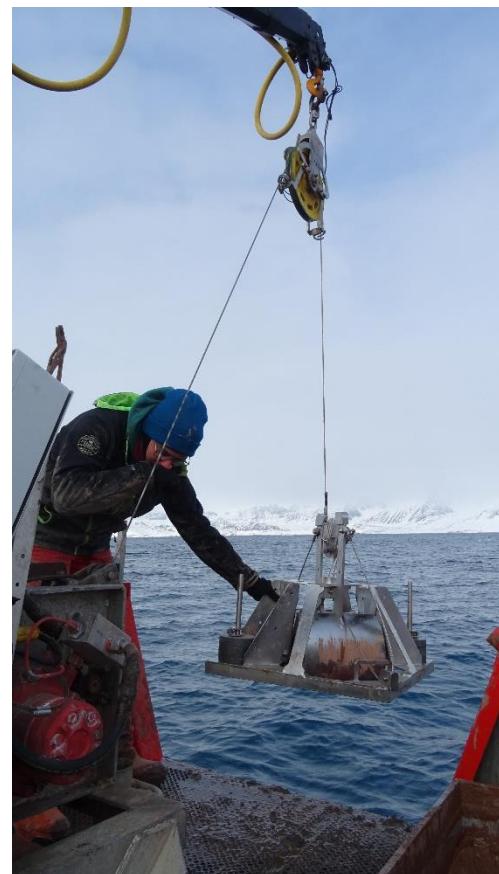
Conversely, sieving the coarse fraction of the sediment (with a diameter greater than 50 μm , or 10 μm in the case of underwater sieving) provides

values corresponding to the actual grain size. However, it is necessary to correct this value by expressing the grain size in terms of the nominal diameter (x_n), where $x_n = 1.15x_v$ is the sieve void. Rivière emphasizes the importance of this nominal diameter concept, as the hydraulic behavior of grains with a given nominal diameter is nearly equivalent to that of a sphere with the same diameter, roughness, and density.

For grain sizes up to $90 \mu m$, the terminal fall velocity can be directly calculated using Stokes' law based on the nominal diameter. However, for diameters exceeding $90 \mu m$, Stokes' law becomes inapplicable. In such cases, Rivière recommends using the Berthois-Gendre formulas to calculate the terminal fall velocities at $20^\circ C$.

$x_n \leq 0.009 \text{ cm}$	$W = 5403(2.65 - 1)x_n^2$
$0.009 \leq x_n \leq 0.052$	$W = 334x_n^{1.309}$
$0.052 \leq x_n \leq 0.152$	$W = 67.795x_n^{0.761032}$
$0.152 \leq x_n \leq 2.043$	$W = 43.33x_n^{0.52819}$
$x_n = \text{nominal diameter}$ (cm)	$W = \text{falling speed limit}$ (cm/s)

Fig. 28 Day Grab N/O Teisten, Ny-Ålesund polar base, 2021
courtesy of A. Baltzer, Univ. Nantes



Tab. 3 Conversion of experimental diameters (mesh void) to Stokes-Berthois diameters (Rivière and Vernhet, 1973)

Experimental diameter (μm)	30	50	100	200	500	1000	5000	10000	20000
Stokes-Berthois diameter (μm)	35	57	108	170	290	380	590	720	860

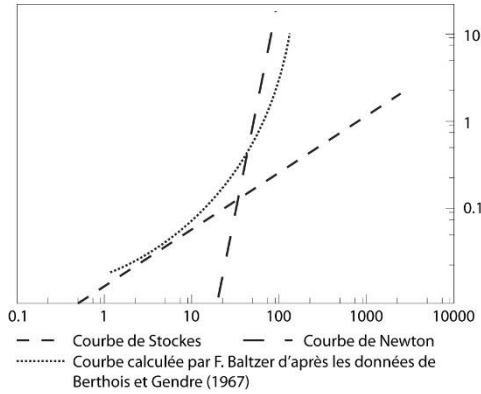


Fig. 29 Falling speed as a function of diameter for quartz spheres in water at 20°C

To express the dimensions of the granulometric fraction subjected to sieving in terms of equivalent dimensions, Stokes' formula can be applied to the previously calculated terminal fall velocities. This yields:

$$\begin{aligned}
 x_n &\leq 0.009 \text{ cm} & X &= X_v + 0.0607 \\
 0.009 &\leq x_n \leq 0.052 & W &= 0.6545X_v + 1.3993 \\
 0.052 &\leq x_n \leq 0.152 & W &= 0.38051X_v + 2.6803 \\
 0.152 &\leq x_n \leq 2.043 & W &= 0.2641X_v + 3.2746
 \end{aligned}$$

X = equivalent diameter, Δ scale X_v = mesh void diameter, Δ scale

In summary, the numerical expression for sieved particles, in equivalent dimensions, requires the following operations:

1. Calculation of nominal diameters x_n ,
2. Calculation of limiting fall velocities W (Berthois-Gendre formulas)

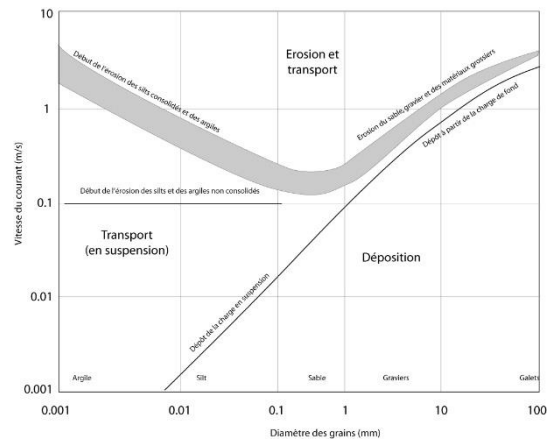


Fig. 30 Hjulstrom diagram. Relationship between grain size, flow velocity and type of sediment movement (sediment density: 2.65 g/cm^{-3})

Tab. 4 Sieve mesh equivalents AFNOR and $X\Delta$

Mailles en mm ($\sqrt[10]{10}$)	$X\Delta$
4	4.754
2.5	4.674
1.6	4.649
1.25	4.620
1	4.583
0.8	4.546
0.63	4.506
0.5	4.468
0.4	4.411
0.315	4.343
0.25	4.278
0.2	4.214
0.16	4.151
0.125	4.081
0.1	4.017
0.08	3.954
0.063	3.860
0.05	3.760
0.04	3.663

4.4 Granulometric Index Method

In 1952, Rivière developed a method to express any granulometric curve using a mathematical equation of the form $y = a x^{\mathcal{N}} + b$. Since then, several calculation methods have been proposed to define \mathcal{N} , and the dynamic significance of this parameter has been further clarified. It quickly became evident that the value of \mathcal{N} , which quantifies the concavity or convexity of the granulometric curve, accurately reflects the energy level present during sediment transport and deposition.

The \mathcal{N} evolution method requires successive determination of the parameters \bar{x} (mean), \mathcal{G} (grading index), and v (a parameter used to determine $\mathcal{N}\mathcal{G}$). This graphical and numerical method is structured as follows:

1. Plotting the Particle Size Curve: Plot the entire particle size distribution curve, expressed in

equivalent dimensions. For the coarse fraction analyzed by sieving, apply corrections using the table of actual dimensions converted into equivalent dimensions

2. Delimiting the Curve Range: Define the integration range of the curve. The upper limit is $x < 0.063 \mu m$ (or 0.8Δ) for the abscissa. The lower limit, y_{inf} , corresponds to the cumulative percentage at $0.063 \mu m$, and the upper limit, y_{99} , corresponds to the cumulative percentage at 99% for the ordinate
3. Integrating the area S in square centimeters
4. Measuring y_{cm} : $y_{cm} = y_{99} - y_{inf}$
5. Calculating $x_{cm} = \frac{S}{y'}$
6. Transforming into reduced mean: Convert x_{cm} into the reduced mean, $\bar{x}r$

$$\bar{x} = \frac{x}{4} \text{ en } \Delta$$

7. Calculation of \bar{x} (mean)

$$\bar{x} = \bar{x}r + 0.8 \text{ en } \Delta \left(\log \frac{6.3}{100} = 0.8\Delta \right)$$

8. Measurement from \mathcal{G} to Δ

$$\mathcal{G} = (x_{99} - 0.8) \text{ en } \Delta$$

9. Measurement of v

$$v = 20 \log \left(\frac{\mathcal{G}}{\bar{x}r} - 1 \right)$$

10. Graphical determination of $\mathcal{N}\mathcal{G}$ from Rivière's abacus (1977)

11. Calculation of \mathcal{N}

$$\mathcal{N} = \frac{\mathcal{N}\mathcal{G}}{\mathcal{G}}$$

12. Graphical representation on a $\bar{x} - -\mathcal{N}$ diagram

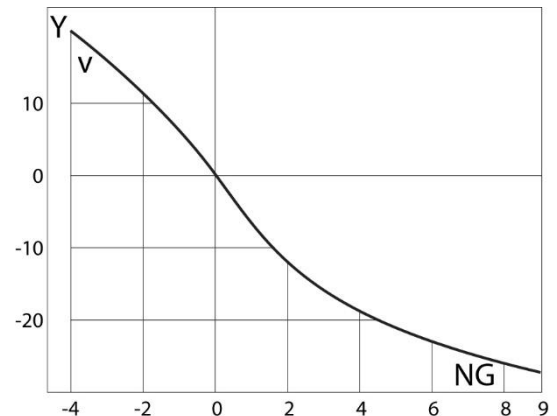


Fig. 31 Graphical determination of the global evolution index \mathcal{O} as a function of \bar{x} et x_{100}

Parametric function

$$x = \mathcal{N}G \text{ et } y = 20 \log \left(\frac{x_{100} - 0.8}{x - 0.8} - 1 \right)$$

4.5 Image processing

The characterization of a sediment and its constituent particles (clasts) relies heavily on the quantitative analysis of their shape, known as morphometric analysis. In this context, geosciences are similar to medical sciences, where image processing techniques are extensively used. Various commercial and open-source software packages are available for this purpose, with ImageJ being one of the most widely used tools. The first review of the application of image processing in sedimentology

was published in 2005 (Francus, 2005). Image processing methods can be divided into several stages:

1. **Sample Preparation and Image Acquisition:** Prepare the sediment sample and acquire images for analysis.
2. **Image Calibration, Filtering, and Metadata Organization:** Calibrate the images, apply necessary filters, and organize metadata.
3. **Measurement Techniques and Error Estimation:** Use measurement techniques to extract metrics and estimate potential errors. The software aims to automatically and quickly measure as many parameters as possible.

Chapter 5 Other Conventional Analyses

5.1 Grain Shape

The formulas for calculating the primary grain shape parameters are provided below. Example graphs are shown in Figures 32 to 36, below.

5.1.1 Sphericity

Two-dimensional sphericity indices are given by Wadell (1935).

$$\varphi_w = \frac{d_c}{D_c}$$

And Riley (1941).

$$\varphi_r = \left(\frac{D_i}{D_c}\right)^{1/2}$$

with d_c the diameter of the nominal cross-section (diameter of a circle with an area equal to the projection of the particle), D_c the diameter of the smallest circumscribing circle, D_i the diameter of the inscribed circle. These indices are based on measurements of the maximum cross-sectional area.

Three-dimensional sphericity indices are given by Krumbein (1941).

$$\psi_i = \left(\frac{BC}{A^2}\right)^{1/3}$$
$$\psi_k = \left\{\left(\frac{B}{A}\right)^2 \frac{C}{B}\right\}^{1/3}$$

And Sneed & Folk (1958).

$$\varphi_p = \left(\frac{C^2}{AB}\right)^{1/2}$$

Where A is the length of the major axis, B the length of the median axis and C the length of the minor axis.

5.1.2 Flattening and Bluntness

The bluntness index is given by Wentworth (1919).

$$F_{wl} = \frac{(A+B)}{2C}$$

Flattening indices are given by Wentworth (1919).

$$F_{w2} = \frac{(A+B+C)}{3}$$

And Cailleux (1947).

$$F_c = \frac{(A+B)}{2C} \times 100$$

Where A is the length of the major axis, B the length of the median axis and C the length of the minor axis.

5.1.3 Lengthening

A two-dimensional index was provided by Dapples and Rominger (1945).

$$E_p = \frac{W_p}{p}$$

And a three-dimensional index by Scheiderhohn (1954).

$$E_s = \frac{B}{A}$$

With W_p the width of the particle projection, L_p the length of the particle projection, A the length of the major axis and B the length of the median axis.

5.1.4 Roundness

These indices are given by Wentworth (1933).

$$P_s = \frac{r_s}{D}$$

Cailleux (1947).

$$P_i = \frac{2r_s}{A}$$

Wadell (1933).

$$P_d = \frac{\sum \frac{r}{R}}{N}$$

And Ouma (1967).

$$X = \frac{3\bar{r}}{(A + B + C)}$$

with r_s the radius of the smallest angle, r the radius of each angle, \bar{r} the mean radius of each angle, R the radius of the largest circumscribed circle, D the radius of the mean grain = $\frac{(A+B)}{4}$ with A the length of the major axis and B the length of the median axis, N the number of angles of the particle (Wadell and Ouma measurements impose the measurement of all angles).

5.1.5 Miscellaneous

The shape index provided by Fleming (1965).

$$\begin{aligned} \text{true or approximate nominal diameter : } D_e \\ = (ABC)^{1/3} \end{aligned}$$

Folk (1974).

$$\text{volume, } V = \left(\frac{\pi}{6}\right) ABC$$

$$\text{maximum projection area, MPA} = \left(\frac{\pi}{4}\right) AB$$

Rivière & Ville (1967).

$$\text{morphological index, } K = \frac{1}{3} \left(\frac{A}{C} + \frac{2r}{C} + \frac{B}{C} \right)$$

with A the length of the major axis, B the length of the median axis, C the length of the minor axis and r the radius of the smallest angle. It is also possible to visually characterize the bluntness of a grain.

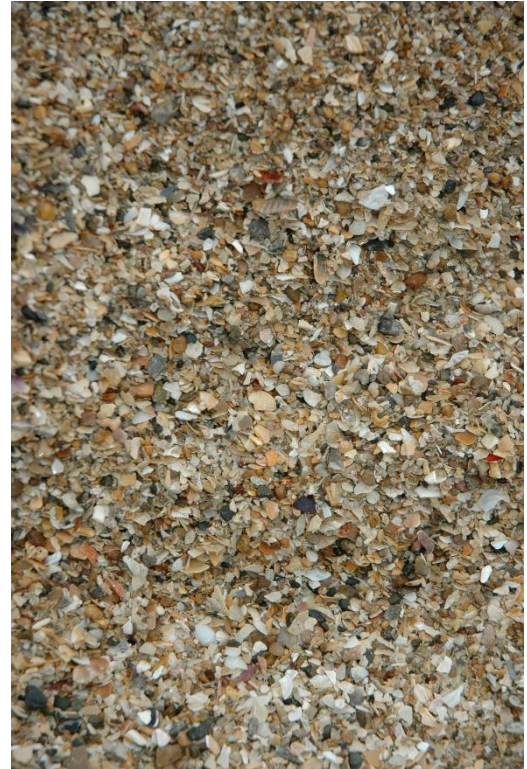
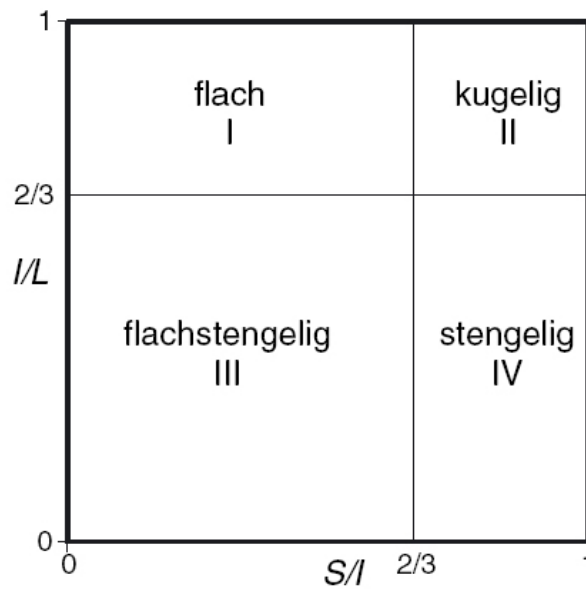
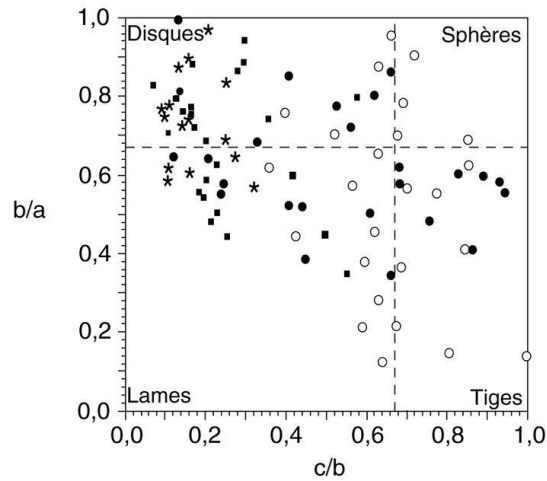
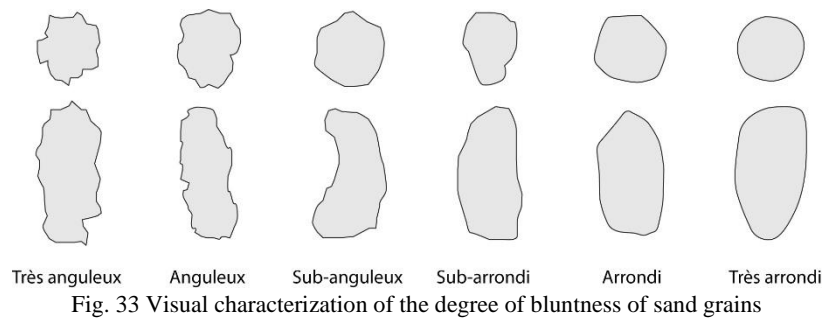


Fig. 32 Highly bioclastic sediment in Mont Saint-Michel bay



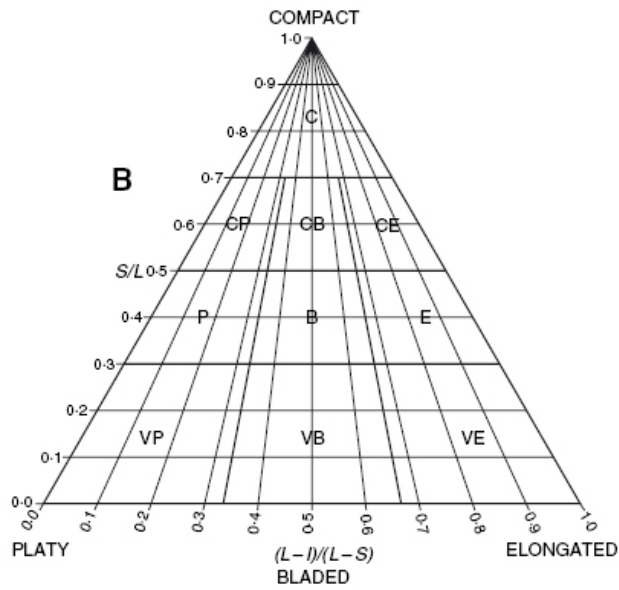


Fig. 36 Sneed & Folk diagram. 10 classes: C (compact), CP(compact-platy), CB (compact-bladed), CE (compact-elongate), P (platy), B (bladed), E (elongate), VP (very platy), VB (very bladed), VE (very elongate) (Sneed & Folk, 1958)

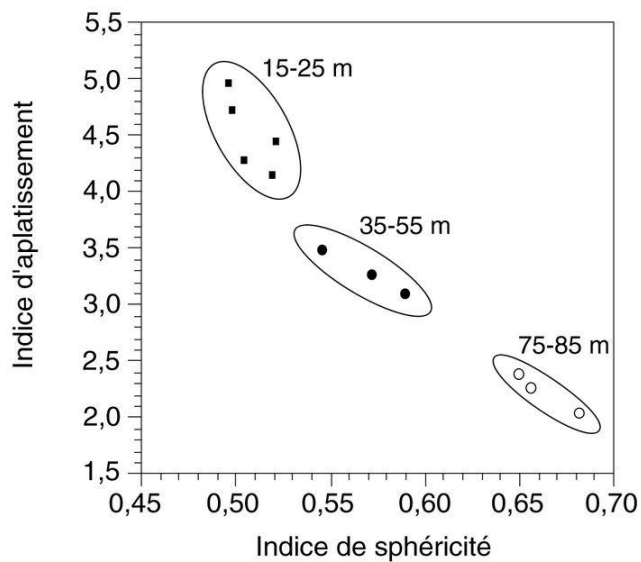


Fig. 37 Relationship between sphericity and kurtosis indices. Each point represents a sample site (average of elements) (Germain and Filion, 2002. Géogr. Phys. Quat., 56(1):81-95)

5.2 Calcimetry

Calcimetry consists in determining the volume of CO_2 released by the action of hydrochloric acid (HCl) on calcium carbonate ($CaCO_3$) in a sample. In all cases, the temperature and atmospheric pressure conditions in the room where the analysis is carried out must be known and controlled.

5.2.1 Sample preparation

1. Pour a saturated solution of sodium chloride ($NaCl$) (approx. $\frac{1}{4}$ l) halfway up the ampoule,
2. Tare the balance and weigh the sample,
3. Check that the sample weight does not exceed 0.4 g,
4. Place sample in Erlenmeyer flask,
5. Place the small tube in the Erlenmeyer flask (the tube must be straight; glue it if necessary). There are also rare models of Erlenmeyer flasks with an inverted finger, known as culture flasks. HCl is then poured directly into the inverted finger, then the Erlenmeyer is tilted so that the HCl flows over the sediment,
6. Using a pipette, pour HCl into the small tube,
7. Stopper the Erlenmeyer flask.

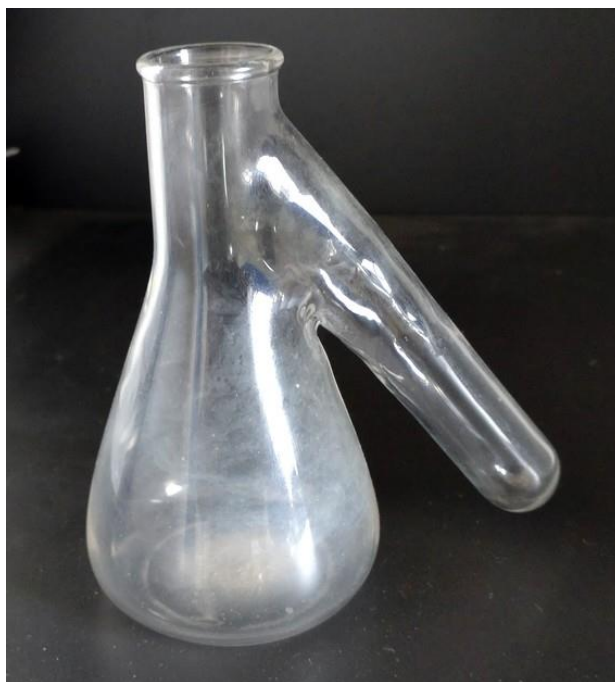


Fig. 38 Specific model of Erlenmeyer for calcimetry

5.2.2 Operating mode (see Fig. 38, below)

1. Change the height of the bulb so that the salt water is at the same level in the bulb and the graduated tube (the Erlenmeyer flask contents will be at atmospheric pressure),
2. Note the level,
3. Tilt the Erlenmeyer to pour the hydrochloric acid onto the sample,
4. Replace the Erlenmeyer flask and wait for the reaction to finish and for thermal equilibration,
5. The pressure in the graduated tube is higher than atmospheric pressure,
6. Re-establish atmospheric pressure by lowering the ampoule until the same level is reached in the ampoule and tube,
7. The CO_2 is at atmospheric pressure, and the measurement can be carried out,
8. Open the Erlenmeyer flask and add a little acid to the sample to check that all the $CaCO_3$ has been attacked.

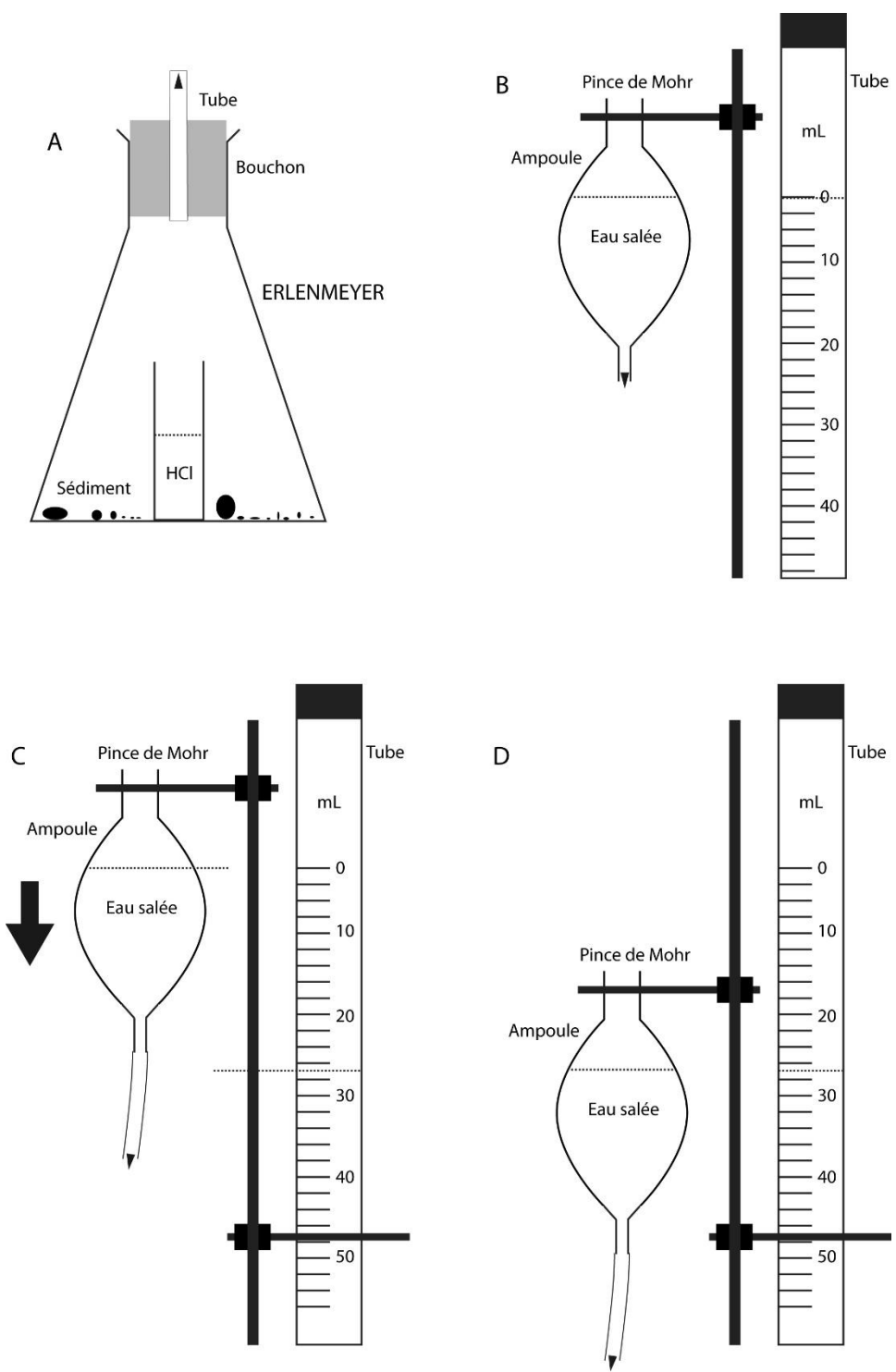


Fig. 39 Calcimetry operations

5.2.3 Calculation of $CaCO_3$ content



As HCl is in excess, its action on one mole of $CaCO_3$ (100 g/mol) releases one mole of CO_2 (22400 mL). Knowing the volume of CO_2 released (final and initial levels), we calculate the mass of $CaCO_3$ attacked. Knowing the mass of $CaCO_3$ and the mass of the sample, we can calculate the percentage of $CaCO_3$ in the sample (Tab. 5).

Tab. 5 Example of calculation method

Mass of $CaCO_3$	Volume of CO_2	
100 g	22400 mL	$x = \frac{(25 \times 100)}{22400}$
x g	25 mL	$x = 0.11$
Mass of $CaCO_3$	Sediment mass	
0.11 g	0.50 g	$y = \frac{(0.11 \times 100)}{0.50}$
y g	100 g	$y = 22.0$

It is strongly recommended to perform several measurements on the same sample in order to accurately estimate the $CaCO_3$ content of a sample by calculating the confidence interval (95%) of the mean.

5.3 Organic Matter

Organic matter (OM) can be estimated using the constant ratio $\frac{\%MO}{\%C} = 1.724$. The OM content is typically determined using the loss on ignition method. However, this method is not recommended for samples with high carbonate content. The calibration range for this method varies from 1% to 50% OM.

5.3.1 Operating mode

1. Grind the sample with a pestle in a mortar. Fragments should be smaller than 2 mm.)

2. Dry the sample for 16 hours at 150°C,
3. Clean porcelain crucibles, heat to red-hot and leave in a desiccator,
4. Weigh the empty crucible,
5. Add sediment (max 10 g) and reweigh the filled crucible,
6. Calcinate 16h in a muffle furnace at 375°C,
7. Cool in a desiccator and weigh the crucible with the ashes.

5.3.2 Calculation of OM content

The results are calculated using the following equations:

$$\begin{aligned} \%OM &= \left(\frac{\text{dry sed. weight (g)} - \text{weight of incinerated sed. (g)}}{\text{dry sed. weight (g)}} \right) \\ &\times 100 \\ \%OM &= \left(\frac{(P_1 - P_0) - (P_2 - P_0)}{(P_1 - P_0)} \right) \times 100 \end{aligned}$$

with P_0 , the mass of the empty crucible, P_1 the final mass, P_2 , the mass of the crucible containing the ashes.

A regression model allows equivalence between the results of the Loss on Ignition (LOI) and Walkley Black (WB) methods for a range of 0 to 8% OM.

$$\%OM (LOI) = 0.9932 \times OM (WB) + 0.587$$

5.4 Water Content

The water content of a sediment sample varies depending on factors such as grain size, sediment composition (e.g., clay content), temperature, and air humidity. Measuring the water content in samples from the intertidal zone can be particularly challenging due to the potential for re-drying. This re-drying is directly related to the time elapsed since

the sediment was exposed, as well as environmental factors like air temperature and wind speed, which can accelerate the drying process.

5.4.1 Dosage

The wet sediment is first weighed and then placed in an oven at 105°C for 24 hours. After drying, the sediment is weighed again. The water content can then be calculated from the difference in weight.

Water content

$$= \left(\frac{\text{wet sample weight} - \text{dry sample weight}}{\text{dry sample weight}} \right) \times 100$$

5.4.2 Concentration calculation for wet sediment

1. wet sediment weighed (WWS),
2. Oven drying (105°C) for 24 h, then weighing of the dry sediment (WDS),
3. WWS – WDS = Weight or volume of water contained in this solution.

The density of the sediment (sand-mud) is assumed to be 2.5. A dry sediment sample weighing x grams occupies a volume of $x/2.5$ =Volume of sediment. In a sediment solution, both the volume of water and the volume of sediment are present. To find the concentration, divide the weight of the dry sediment by the sum of these two volumes and then multiply by 1000 to convert to the volume of a liter of water.

Wet sediment weight	Dry sediment weight	Sediment volume	Water volume	Total volume solution
61.2934	30.124	12.05	31.17	43.22

Concentration: $\frac{(30.124 \times 1000)}{43.22} = 697 \text{ g/l}$. To obtain a concentration of 100 g/l, take $\frac{(100 \text{ g} \times 1000 \text{ cc})}{697 \text{ g}} = 143.47 \text{ cc}$ of solution and make up to 1 l.

5.5 Settling and Rheology of Silts

5.5.1 Granulometric, mineralogical and chemical characteristics of muddy sediments

Pelitic or lutite sediments are less than 40 μm in size. Fine sediments can be broadly classified as follows:

- Silts. From 100 to 10 μm . Low compaction of the deposit base,
- Silts. From 40 to 2 μm . Settling completed in a few days,
- Clays. < 2 μm . Corresponds to a particular mineralogical variety,
- Sludge. Earth and/or dust of terrestrial origin mixed with water,
- Powders. Finely ground solid substances. Mixed with water, they form substances with properties similar to those of silts or sludges, but with one element dominating their composition,
- Tangué. Sediment deposited in certain intertidal mudflats, dominated by a carbonate fraction of bioclastic origin (very finely crushed shellfish debris or phycogenes - maerl) and a silty and/or clayey fraction,
- Mud. Generic term for very fine materials with a high percentage of colloids and abundant organic matter. They take a very long time to settle and their rigidity (or cohesion) varies rapidly with their water content.

5.5.2 Falling speed and particle flocculation

Settlement studies are carried out on fractions < 40 μm or pure silt, or on mixtures with increasing percentages of silts and fine sands. Suspension takes place in water of increasing salinity or in the original water.

Particles 30 μm in size fall at around 1 mm/s. Average diameters range from 1/10th of a μm to around ten μm for certain silts (Tab. 6). The finest marine silts have a hyperbolic curve (settling in calm zones), while river sediments have a parabolic curve (excess load).

Tab. 6 Falling speed vs. Sediment size

0.00001	0.0001	0.001	0.01	0.1	1	Falling speed mm/s
0.1	0.3	1	3	10	30	Equivalent particle diameter

Equatorial marine vases, which are rich in kaolinite, exhibit hyperbolic-index shapes. Temperate marine muds, primarily composed of illite, kaolinite, and smectite, typically display logarithmic profiles. Estuarine muds often show either logarithmic or parabolic profiles.

Coarse elements such as sand, gravel and pebbles behave individually in aqueous media. Silt and mud, on the other hand, are subject to flocculation, a phenomenon that contributes to the formation of aggregates whose falling speed is greater than that of the elementary particles. The specific surface is the lateral surface of the unit mass. A material volume of 1 cm^3 of 1 μm particles would represent a developed surface area of 4.20 m^2 , assuming a void index of 30%. Stockes' law describes the speed of fall:

$$W = \frac{1}{18} \cdot \frac{\rho_s - \rho_o \cdot d^2 g}{\rho_o \cdot \nu}$$

with ρ_s the specific mass of the particle in kg/m^3 ; ρ_{so} the kinematic mass of water in m^2/s (or in stock cm^2/s) ($\nu = 1.10^{-6} \text{ m}^2/\text{s}$ at 20°C for pure water and $1.6 \cdot 10^{-3} \text{ m}^2/\text{s}$ for pure water at 4°C), d the particle's equivalent diameter.

If a particle of density 2.5 to 2.6 falls into soft water at 20°C (viscosity = $1.10^{-6} \text{ m}^2/\text{s}$), the ratio between the equivalent diameter in μm and the falling speed in μ/s is given by $d_{\mu\text{m}} = W^{1/2} \mu\text{m}$. Flocculation increases as :

- electrolyte concentration increases,
- ion values increase,
- temperature increases,
- hydrated ion size decreases,
- the dielectric constant decreases,
- pH decreases,
- the absorption capacity of anions decreases.

A suspension of sludge in water will flocculate all the better if :

- the elementary particles are smaller,
- their concentration in the suspension will be high,
- the medium will contain high levels of flocculant salts,
- water temperature is high.

The average falling velocity of silt in its deflocculated state (in the form of elementary particles) in pure water is between 10^{-5} and $10^{-1} \text{ mm}/\text{s}$. In seawater, for a solid particle concentration of 10 g/l , the average falling velocity of flakes is between $1.5 \cdot 10^{-1} \text{ mm}/\text{s}$ and $6 \cdot 10^{-1} \text{ mm}/\text{s}$, i.e. a ratio of 1 to 4. The flocculation factor is:

$$F = \frac{W_f 50\%}{W_p 50\%}$$

with W be the average settling velocity: W_f of flakes in flocculent aqueous media, and W_{fp} for elementary particles in deflocculated media.

The flocculation factor varies inversely with the equivalent diameter d of the elementary particles. Smaller particles have a higher flocculation factor. For instance, with 10 g/l of dry sediment in seawater at a salinity of 30, $\mapsto F = 250 d^{-2}$. In a flocculent medium, a sludge suspension will have average settling velocities ranging from 0.15 to 0.60 mm/s in calm water, regardless of the size of the elementary particles. However, flocculation becomes ineffective when particle size exceeds 40 μm . If the suspension is agitated, aggregate formation can be accelerated, leading to average flake settling velocities of around 1 to 1.5 mm/s, such as during slack tide in estuaries.

5.5.3 Silt settling

During the settling process, silt initially loses its interstitial water. In a subsequent stage, it loses water from the double layer, which involves the arrangement of solid particles and their adsorbed water. Liquid sludge retains a significant amount of interstitial water. As it transitions to a plastic state, only the double-layer water remains, and it becomes solid when the particles come into direct contact with each other.

Water is expelled uniformly from the surface through upwelling, but preferential drainage wells can form, where coarse elements tend to accumulate. Drainage may also occur at the base or laterally, especially if the silt is situated on permeable sand. The average concentration of a deposit varies logarithmically over time, with different settling domains corresponding to the hindered settling velocity of the flakes.

The concentration (weight of dry particles per volume of mixture) is given by:

$$T_s = \alpha \cdot \log t + \beta$$

with t the settling time, α the factor related to particle diameter, β the factor related to the aqueous medium.

For settlement studies, we use the alpha-densimetric probe to measure the density of deposits at various depths, and the rheological probe to assess the rigidity of these deposits. Mud mixtures (either freshwater or with varying salinities) with concentrations ranging from 5 to 300 g/l are introduced into transparent tubes that are 10 cm in diameter and vary in height from 0.25 to 4 meters. The temperature is maintained at a constant 20°C. Variable percentages of sand and silt can also be incorporated into these mixtures. The alpha-densimeter is used to periodically measure the concentration of the deposits. The characteristics of the deposits are:

- T_s the dry sediment content, i.e. the mass of dry sediment contained in a unit volume of mixture. T_s is expressed in kg/m^3 or g/l ,
- T_e the water content, i.e. the ratio of the weight of water contained in the sample to the weight of dry sediment after study at 105°C. T_e is expressed in %,
- $\frac{\rho_m}{\rho}$ the mixture density, i.e. the ratio between the mass of the mixture volume unit and the density of water at 4°C.

•

$$\frac{\rho_m}{\rho} = 1 + \left(\frac{\rho_s - \rho_o}{\rho_s} \right) \cdot \left(\frac{T_s}{1000} \right)$$

If $\rho_s = 2500 \text{ kg/m}^3$ and $\rho_o = 1000 \text{ kg/m}^3$, then

$$\frac{\rho_m}{\rho} = 1 + 0.6 \cdot 10^{-3} T_s$$

$$Te\% = \left(\frac{\rho_o}{T_s} \right) - \left(\frac{\rho_o}{\rho_s} \right) \cdot 100$$

5.5.4 Physical properties of a solid particle in still water

Depending on the relative motion of the fluid with respect to the particle, the flow can be classified as laminar (Stokes regime), semi-turbulent (Allen regime), or turbulent (Newton-Rittinger regime). These flow regimes correspond to specific ranges of Reynolds numbers, which represent the ratio of inertial forces to viscous friction forces.

For a particle falling through water, the Reynolds number (Re) is given by:

$$Re = \frac{W \cdot D}{\mu}$$

where W is the settling velocity, D is the particle diameter, and μ is the kinematic viscosity of water. At 20°C, μ is $10^{-6} \text{ m}^2/\text{s}$, while at 3.5°C, it is $1.6 \times 10^{-6} \text{ m}^2/\text{s}$.

- Laminar flow: $Re < 1$, $W = KD^2$ ($D < 0.12 \text{ mm}$), mud, silts,
- Semi-turbulent flow: $1 < Re < 500$, $W = KD$ ($0.12 < D < 2 \text{ mm}$), sands,
- Turbulent flow: $Re > 500$, $W = KD^{1/2}$ ($D > 2 \text{ mm}$), gravels, pebbles.

The influence of liquid viscosity, and therefore temperature, must be taken into account. Falling speed can be halved when water temperature drops from 30°C to 4°C.

- Laminar flow: the velocity of fall (cm/s) is $\left(\frac{D}{100}\right)^2$. A 30 μm particle falls at 0.1 cm/s ,
- Semi-turbulent flow: for natural sands of density $\rho = 2.6 \text{ kg/m}^3$, the velocity of fall (mm/s) is $125D$. A 1 mm diameter sand falls at 12.5 cm/s ,

- Turbulent flow: A 50 cm pebble falls at a speed of 2 m/s .

5.5.5 Set of particles

When a large number of particles fall into a liquid, they can get in each other's way, considerably altering the speed of their fall. This is known as impeded velocity. If these particles are fine, they tend to agglomerate and form small flakes. This is known as flocculation.

Impeded falling speed: The falling speed of particles larger than 100 μm decreases with increasing suspension concentration. For example, fine sand at a concentration of 100 g/l falls 0.75 times slower than the elementary particle.

Flocculation of fines: For fine particles, flocculation is the property of generating aggregates much larger than those of elementary particles (aggregates of 0.7 to 2 mm for particles of a few μm). A 1 μm elementary mud particle has a falling speed of 0.001 mm/s , i.e. it takes 12 days to travel 1 m in height in still water. In the flocculated state, its falling speed is between 0.1 and 0.8 mm/s . This is multiplied by a factor of 100 to 800 (on average by a factor of 500), so it will take only 2000 seconds, or 1/2 an hour, to travel 1 m through the water. Falling speed increases:

- With increasing concentration between 0 and 20 g/l , the impeded fall velocity initially increases but then diminishes. This velocity rises from 0.02 to 0.2 mm/s , a tenfold increase.
- With salinity, the falling speed increases as salinity rises from 0 to 5, after which it remains constant. At a concentration of 2 g/l , the fall rate increases from 0.05 mm/s to 0.5 mm/s at a salinity of 3.

In natural conditions, deflocculated silt has a fall velocity of approximately 0.5 mm/s in calm water. In estuaries, the fall velocity of macroflocs, which

form around slack water during high and low tides, can reach 1 to 2 *mm/s*.

Chapter 6 Sediment Mapping

The aim of a sediment sampling campaign may be to create a sedimentological and/or morpho-sedimentological map. This type of map can represent multiple layers of information simultaneously. The sedimentary cover of a geographical area can be examined by analyzing either its surface (surface cover) or its sub-surface (deposit thickness). The thickness of sedimentary deposits can be estimated using seismic reflection. Sonograms produced through this method can identify and measure the internal structure and strength of unconsolidated sediments, providing insight into their deposition process.

6.1 Map Legend

The map legend typically includes grain size classes based on an established scale (such as Blott and Pye, Folk and Ward, Udden, or Wentworth) or a scale specifically defined for the study. It may also represent textural groups, carbonate percentage,

water content, and organic matter. Depending on the nature of the sediments in the study area and the map's scale, grain size classes might need to be merged (for highly heterogeneous areas) or subdivided (for very homogeneous areas) (see Augris & Clabaut, 2001 ; Augris et al., 1996, Boillot et al., 1974 ; Fournier et al., 2009, 2010 ; Larsonneur, 1977, Vaslet et al., 1979).

The main types of sedimentary maps include:

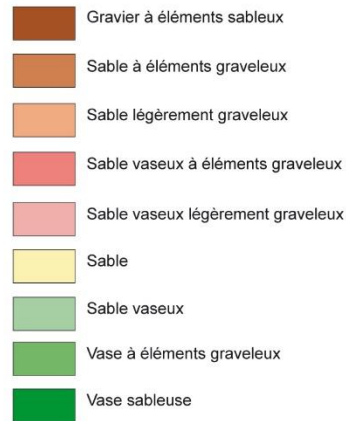
- Morpho-sedimentological map
- Sedimentary figure map
- Sedimentary facies map
- Carbonate content distribution map
- Surficial formations map
- Textural group map

Maps can be divided into two groups: those that focus on the morphology and nature of the seabed, and those that focus on the distribution of sediments or carbonate content.

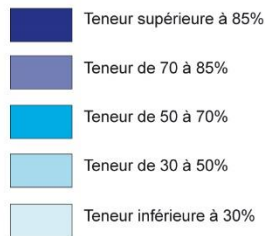
Faciès sédimentaires (modifiés selon Wentworth, 1922)



Groupes texturaux (Folk & Ward)



Distribution quantitative du calcaire (CaCO₃)



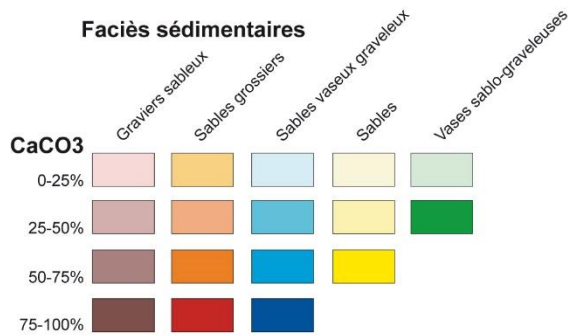
Faciès sédimentaires couvrant le domaine intertidal



Figures sédimentaires du domaine intertidal



Faciès sédimentaires



Figures sédimentaires

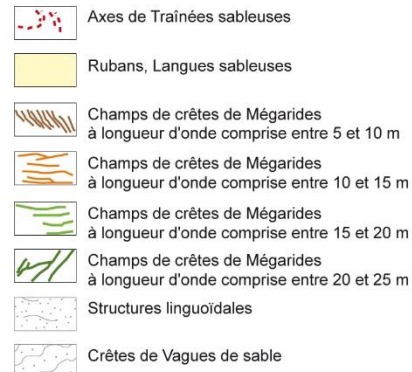


Fig. 40 Some examples of legends (in French) used on sedimentology maps

6.2 Seabed Types

Seabed maps can be used to distinguish between rocky and sedimentary seabeds. They provide detailed descriptions of the main sedimentary assemblages or facies, such as bio- or lithoclastic compositions, the presence of shell debris, and phycogenes, and can categorize areas into domains like infralittoral and intertidal.

Sediment maps are created using bathymetric echosounder and sidescan sonar imagery. These maps allow for the identification and spatial analysis of the architecture and orientation of sediment accumulation features. Generally, these features can be classified into two categories based on their orientation relative to the dominant direction of sediment transport. When oriented parallel to the dominant direction, they are termed longitudinal figures; when perpendicular, they are known as transverse figures.

- Longitudinal patterns include sandbanks of varying amplitudes, which can extend for several kilometers. These features are often shaped by transverse structures such as ripples and mega-ripples. Other examples of longitudinal patterns are sandy streaks, sandy ribbons, tongues, and comet tails.
- Transverse figures comprise features like mega-waves with wavelengths exceeding a meter and sand waves that have a maximum amplitude of several meters and very long wavelengths (over a hundred meters). This category also includes beach crescents and foreshore bars.

6.3 Sedimentary Facies

Surficial sediment distribution maps are based on granulometric data, which detail the sediment's composition, including both a detrital lithogenic phase and a carbonate biogenic phase. Conventional indices are used to determine the average grain size, identify the main or dominant particle size phase, and classify the sediment (e.g., *So Trask*). Facies can then be defined accordingly.

It is advisable to systematically indicate the size class corresponding to each facies (e.g., silts and fine sands, 40 to 200 μm). In cases where the study area contains multi-modal sediments, subdividing facies based on the predominance (> 75-80%) or dominance (50-60%) of each granulometric fraction may be necessary. This can lead to the identification of intermediate facies. For instance, a sediment with 40% coarse sands, 40% medium sands, and 20% fine sands might be represented by an intermediate class of coarse and medium sands.

In some cases, sediments may be highly heterogeneous, consisting of gravel, coarse sand, and mud. These sediments are often very biologically rich.

Carbonate content distribution maps can be shown separately or in conjunction with the main facies maps. When combined, a cross-referenced legend is required for accurate interpretation. If the nature of the carbonate phase is known (e.g., whole shells, debris, bivalves, gastropods, maerl, etc.), it can be represented on the map. This level of detail is not feasible for some types of carbonate content, such as carbonate-rich mud (tangué).

The relative percentages of different bioclast types can be estimated visually from photographs and plotted accordingly.

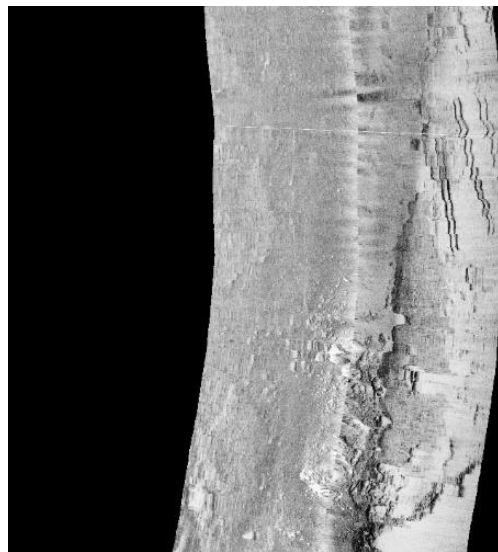
6.4 Operating Mode

To create a sedimentological map, it is advantageous to use aerial or acoustic imagery, such as that obtained from side-scan or multibeam sonar. Interpreting these images allows for the identification and mapping of the main visible structures and the delineation of the most characteristic facies, at least approximately, in terms of structure and texture. These homogeneous areas are referred to as isophenes. For example, an area characterized by ripple-marked medium sands can be easily delineated using this method (Fournier et al., 2010).

Fig. 41 EdgeTech acoustic sonar on board the N/O Serpula Heriot-Watt University, Edinburgh



Fig. 42 Acoustic image



A sampling strategy can then be chosen according to a stratified design. This method is particularly recommended for highly heterogeneous areas such as archipelagos. If the study area appears to be particularly homogeneous, such as certain bays, a regular grid plan should be adopted, with the grid spacing defined based on logistical and scientific criteria. In the field, samples are systematically geo-referenced using GPS to ensure that each facies or morphological change is accurately located. Photographs of the sediment are also very useful for determining sediment classes (bare sediment, algae-colonized or not, with shell deposits, etc.). These pieces of information (images, photographs, coordinates x , y , and z , grain size curves, quantitative and qualitative data, etc.) can then be incorporated into a Geographic Information System (GIS). Finally, the maps themselves are produced using vector graphic software.

The Chausey Archipelago (Normandy), located in the Normand-Breton Gulf, recently underwent an extensive morpho-sedimentological mapping campaign of its intertidal zone. Some maps are provided in Chapter 7 below.

Chapter 7 Sedimentological Maps

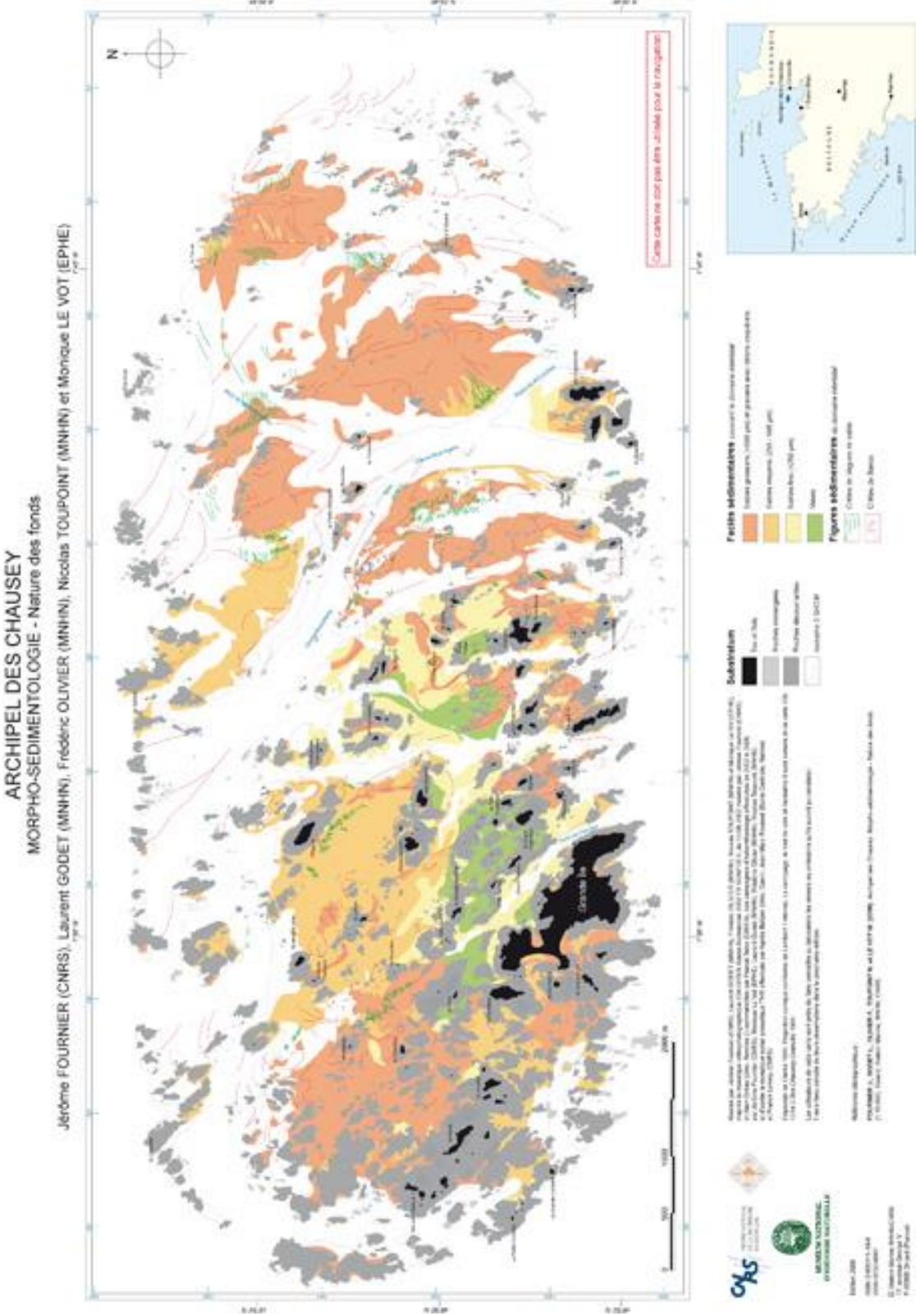


Fig. 43 Morpho-sedimentological map, Chausey Archipelago, Normandy, France

ARCHIPEL DES CHAUSEY
 REPARTITION DES SEDIMENTS SUPERFICIELS - Distribution du calcaire

Jérôme FOURNIER (CNRS), Laurent GOBET (MNHM), Frédéric OLIVIER (MNHM), Nicolas TOUPOINT (MNHM) et Monique LE VOT (EPHE)

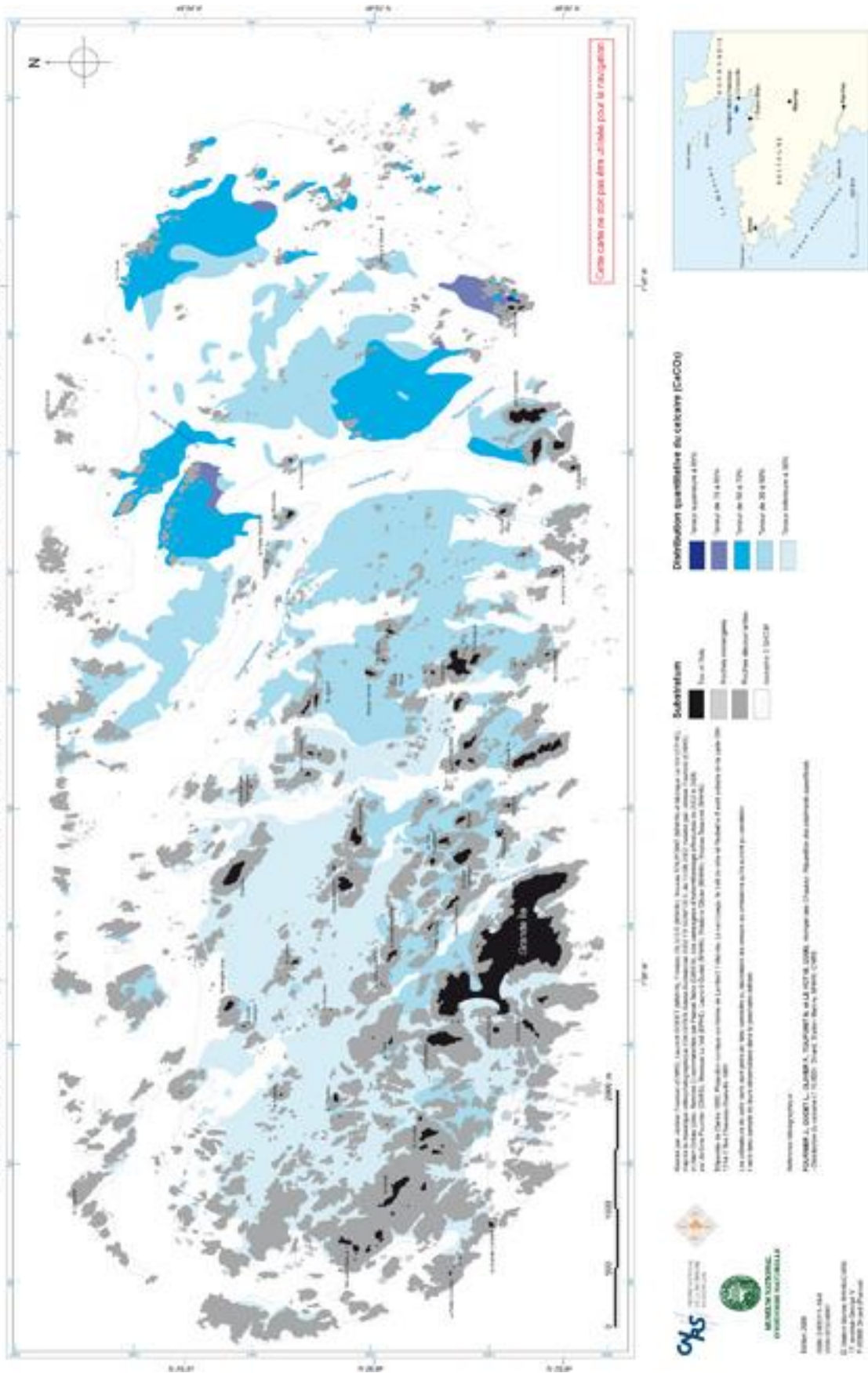


Fig. 47 Carbonate content distribution map, Chausey Archipelago, Normandy, France

ARCHIPEL DES CHAUSEY
REPARTITION DES SEDIMENTS SUPERFICIELS - Groupes texturaux

Jérôme FOURNIER (CNRS), Laurent GODET (MNHM), Frédéric OLIVIER (MNHM), Nicolas TOUPOUR (MNHM) et Monique LE VOT (EPHE)

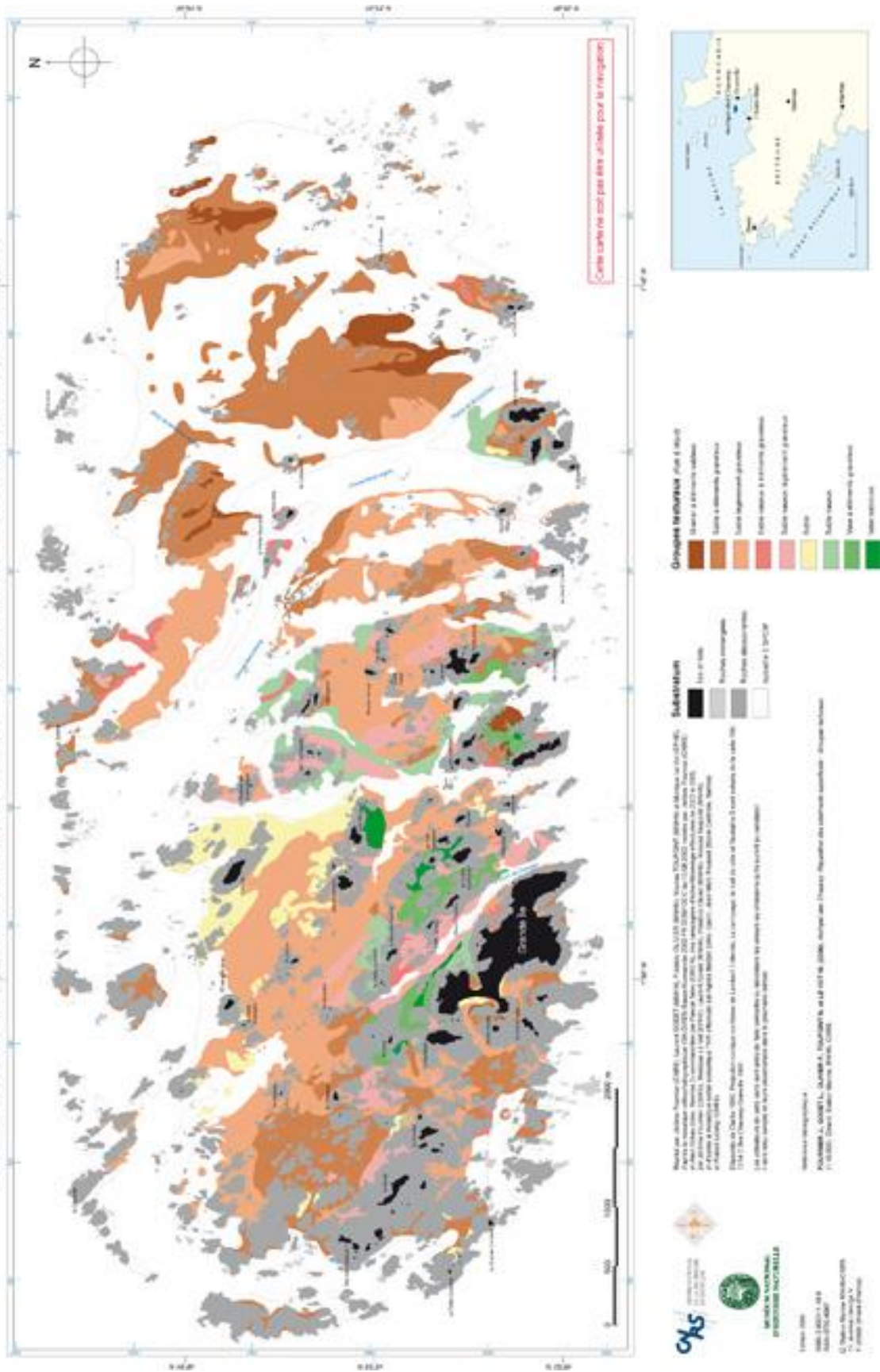


Fig. 48 Textural groups map, Chausey Archipelago, Normandy, France

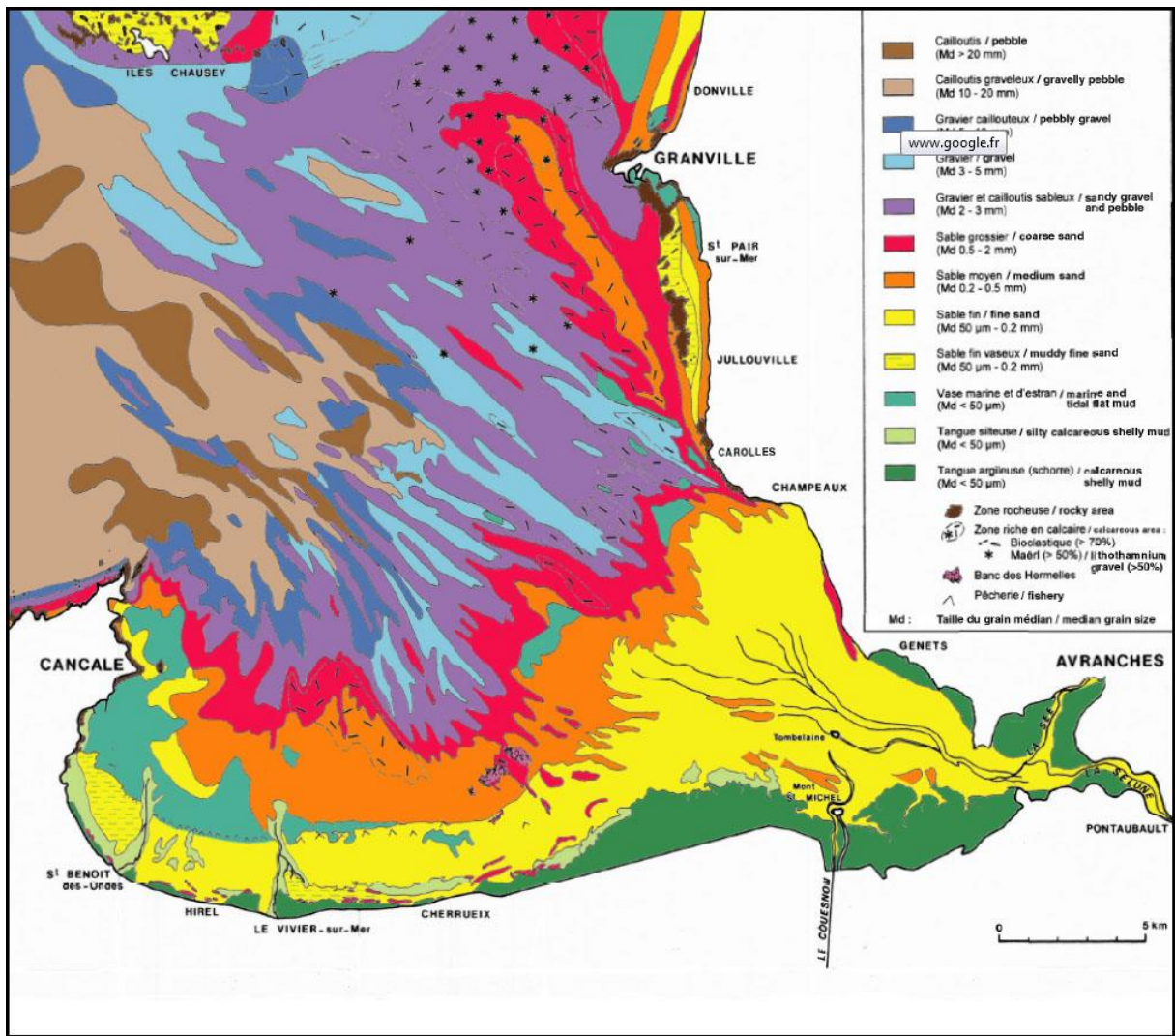


Fig. 49 Sedimentological map, Mont Saint-Michel Bay, France

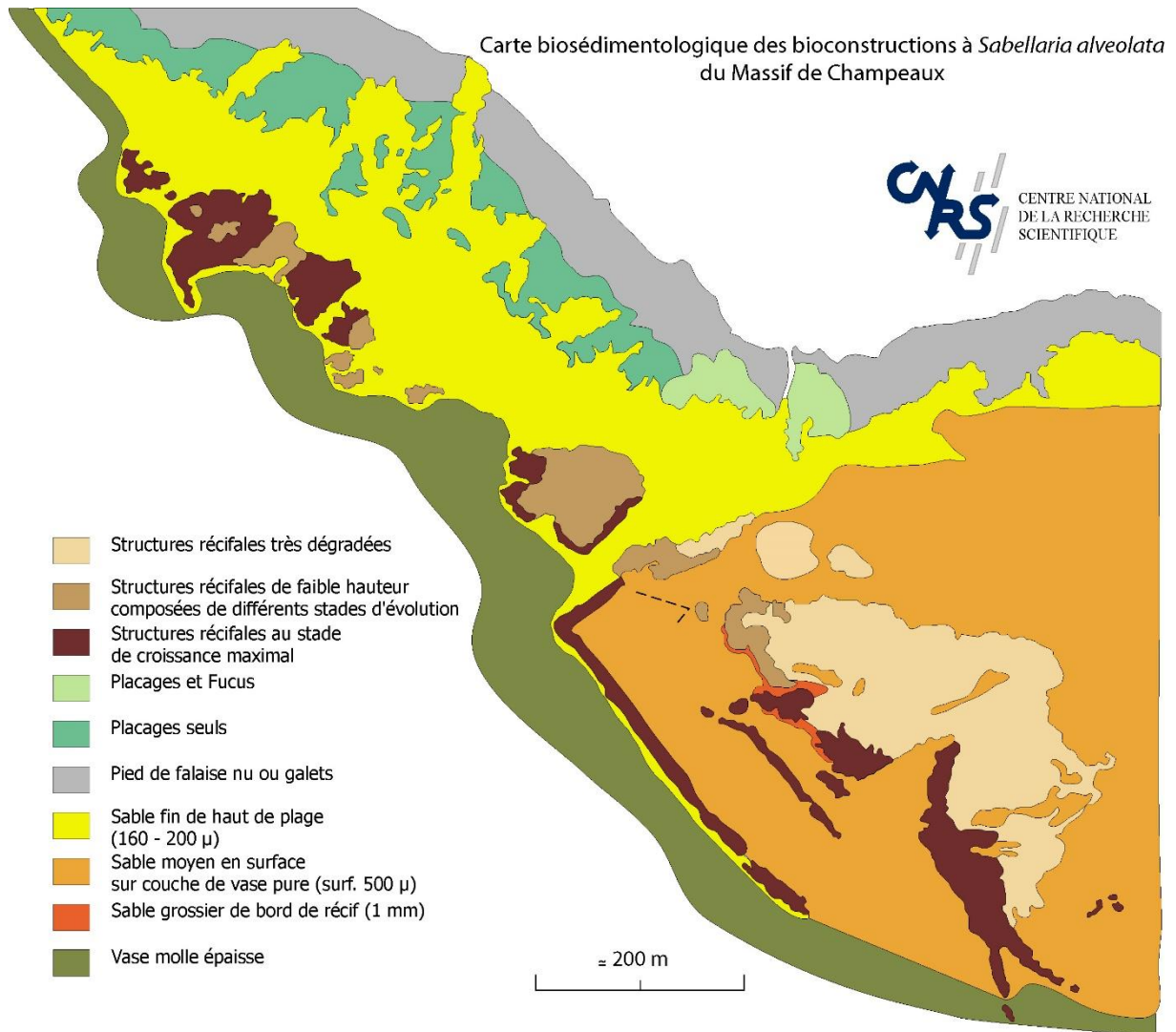


Fig. 50 Biosedimentological map of a honeycomb worm, Mont Saint-Michel Bay, France

Personal notes

Bibliography

AFNOR, *Granulométrie* - 2 volumes, tomes 1 et 2, AFNOR, Paris, 2000

Augris, C., Clabaut, P., *Cartographie géologique des fonds marins côtiers. Exemples le long du littoral français*, Editions IFREMER, Plouzané, 2001

Augris, C., Hamon, D., Mazé, J.P., Bonnot-Courtois, C., Garreau, P., Guénnoc, P., Guénoilé, A., Houlgatte, E., *Atlas thématique de l'environnement marin en baie de Saint-Brieuc*, Editions IFREMER, Plouzané, 1996

Bagnold, R.A., Barndorff-Nielsen, O.E., The pattern of natural grain size distribution. *Sedimentology* 27: 199-207, 2004

Bell, D.F., Loss-on-ignition as an estimate of organic matter and organic carbon in non-calcareous soils. *Journal of Soil Science* 15: 84-92, 1964

Bellair, P., Pomerol, C., *Eléments de géologie*, Armand Colin, Paris, 1977

Beuselinck, L., Govers, G., Poesen, J., Degraer, G., Grain-size analysis by laser diffractometry: comparison with the sieve-pipette method. *Catena* 32:193-208, 1998

Blott, S., Fournier, J., *Gradistat v. 4.1. A grain size distribution and statistics package for the analysis of unconsolidated sediments by $\frac{1}{2} \phi$, $\frac{1}{142} \phi$ or AFNOR sieving or Laser Granulometer*, Royal Holloway University of London, Centre National de la Recherche Scientifique, Dinard, 2004

Blott, S.J., Pye, K., GRADISTAT: a grain size distribution and statistic package for the analysis of uncololidated sediments. *Earth Surface Processes and Landforms* 26: 1237-1248, 2001

Boillot, G., Lefort, J.P., Cresard, A., Musellec, P., *Carte géologique de la Manche au 1/100,000*, BRGM-CNEXO, Orléans, 1974

Bonnot-Courtois C., Fournier J., Dréau A., Recent morphodynamics of shell banks in the western part of Mont Saint-Michel Bay (France), *Géomorphologie : relief, processus, environnement* 04(1), p 65-80, 2004

Cailleux, A., Tricart, J., *Initiation à l'étude des sables et des galets*, 3 tomes, Centre Doc. Univ., Paris, 1959

Campy, M., Macaire, J.J., *Géologie des formations superficielles*, Masson, Paris, 1989

Campy, M., Macaire, J.J., *Géologie de la surface*, Dunod, Paris, 2003

Chamley, H., *Sédimentologie*, Dunod, Paris, 1987

Chamley, H., *Les milieux de sédimentation*, Tec & Doc, Lavoisier, Paris, 1988

Chamley, H., Deconinck, J.F., *Bases de sédimentologie*, Dunod, Paris, 2011

Cheetham, M.D., Keene, A.F., Bush, R.T., Sullivan, L.A., Erskine, W.D., A comparison of grain-size analysis methods for sand-dominated fluvial sediments. *Sedimentology* 55: 1905-1913, 2008

- Cojean, I., Renard, M., *Sédimentologie*, Dunod, Paris, 1999
- Davis, M.W., Ehrlich, R. Relationships between measures of sediment-size-frequency distributions and the nature of the sediments. *Geological Society of America Bulletin* 81: 3537-3548, 1970
- Di Stefano, C., Ferro, V., Mirabile, S., Comparison between grain-size analyses using laser diffraction and sedimentation methods. *Biosystems Engineering* 106: 205-215, 2010
- Dur, J.C., Elsass, F., Chaplain, V., Tessier, D., The relationship between particle-size distribution by laser granulometry and image analysis by transmission electron microscopy in a soil clay fraction. *European Journal of Soil Science* 55: 265-270, 2004
- Folk, R.L., The distinction between grain size and mineral composition in sedimentary-rock nomenclature. *Journal of Geology* 62: 344-359, 1954
- Folk, R.L., A review of grain-size parameters. *Sedimentology* 6: 73-93, 1966
- Folk, R.L., Ward, W.C. Brazos River bar: a study in the significance of grain size parameters. *Journal of Sedimentary Petrology* 27: 3-26, 1957
- Fournier J., Baltzer A., Godet L., Panizza A., Acoustic imagery for benthic habitats mapping and monitoring, Chapter 5, in - *Geomatic solutions for coastal environments* -, eds. M. Maanan & M. Robin, Series Environmental Science, Engineering and Technology, Nova Science Publishers, Inc., New-York, p 141-161, 2010.
- Fournier J., Bonnot-Courtois C., Paris R., Le Vot M., *Analyses granulométriques, principes et méthodes*, CNRS, Dinard, 99 p, 2013
- Fournier J., Gallon R., Paris R., G2Sd: a new R package producing statistics on the distribution of unconsolidated sediments, *Géomorphologie, relief, processus, environnement* 14(1), p 73-78, 2014.
- Fournier J., Godet L., Bonnot-Courtois C., Baltzer A., Caline B., Distribution des formations superficielles de l'archipel de Chausey (Manche), *Géologie de la France*, BRGM, Orléans 1, p 5-17, 2009.
- Francus, P., *Image analysis, sediments and paleoenvironments*, Springer, Berlin, 2005
- Friedman, G.M., Differences in size distributions of populations of particles among sands of various origins. *Sedimentology* 26: 3-32, 1979
- Gallon, R.K., Fournier, J., *G2Sd: Grain-size statistics and description of sediment*. CRAN R-package, 2012
- Gardiner, V., Dackombe, R., *Géomorphological Field Manual*, George Allen & Unwin, London, 1983
- Godet L., Fournier J., Toupoint N., Olivier F. Mapping and monitoring intertidal benthic habitats: a review of techniques and proposal of a new visual methodology for the European coasts, *Progress in Physical Geography* 33(3), p 378-402, 2009.
- Inman, D.L., Sorting of sediments in the light of fluid mechanics. *Journal of Sedimentary Petrology* 19: 51-70, 1949

- Inman, D.L., Measures for describing the size distribution of sediments. *Journal of Sedimentary Petrology* 22: 125-145, 1952
- Koldijk, W.S., On environment-sensitive grain-size parameters. *Sedimentology* 10: 57-69, 1968
- Kondolf, G.M., Sale, M.J., Wolman, M.G. Modification of fluvial gravel size by spawning Salmonids. *Water Resources Research* 29: 2265-2274, 1993
- Kondolf, G.M., Wolman, M.G. The sizes of Salmonid spawning gravels. *Water Resources Research* 29: 2275-2285, 1993
- Konert, M., Vandenberghe, J. Comparison of laser grain size analysis with pipette and sieve analysis: a solution for the underestimation of the clay fraction. *Sedimentology* 44: 523-535, 1997
- Krinsley, D.H., Doorkamp, J.C., *Atlas of quartz sand surface textures*, Cambridge University Press, London, 1973
- Krumbein, W.C., Size frequency distributions of sediments. *Journal of Sedimentary Petrology* 4: 65-77, 1934
- Krumbein, W.C., Size frequency distributions of sediments and the normal phi curve. *Journal of Sedimentary Petrology* 8: 84-90, 1938
- Krumbein, W.C., Pettijohn, F.J., *Manual of Sedimentary Petrography*, Appleton-Century-Crofts, New-York, 1938
- Laboratoire central des Ponts et Chaussées, *Granulométrie*, Bulletin de Liaison des Laboratoires des Ponts et Chaussées, Ministère de l'Équipement et du Logement, Paris, 1988
- Larsonneur, C., La cartographie des dépôts meubles sur le plateau continental français : méthode mise au point et utilisée en Manche. *Journal de la Recherche Océanographique* II(2): 33-39, 1977
- Le Ribault, L., *L'exoscopie ; méthodes et applications*, Notes et mémoires 12, Total Cie française des Pétroles, Paris, 1975
- Mahaney, W.C., *Atlas of sand grain surface textures and applications*, Oxford University Press, Oxford, 2002
- McCammon, R.B., Efficiencies of percentile measures for describing the mean size and sorting of sedimentary particles. *Journal of Geology* 70: 453-465, 1962
- Middleton, G.V., Hydraulic interpretation of sand size distributions. *Journal of Geology* 84: 405-426, 1976
- Miller, F.P., Vandome, A.F., McBrewster, J., *Sédimentologie*, Alphascript Publishing, Mauritius, 2010
- Otto, G.H., A modified logarithmic probability graph for the interpretation of mechanical analyses of sediments. *Journal of Sedimentary Petrology* 9: 62-75, 1939
- Paris R., Cachão M., Fournier J., Voltaire O., Nannoliths abundance and distribution in tsunami deposits: example from the December 26, 2004 tsunami in Lhok Nga (northwest Sumatra, Indonesia), *Géomorphologie : relief, processus, environnement* 10(01), p 109-118, 2010.

Paris R., Fournier J., Poizot E., Etienne S., Morin J., Lavigne F., Wassmer P., Boulder and fine sediment transport and deposition by the 2004 tsunami in Lhok Nga (western Banda Aceh, Sumatra, Indonesia): a coupled offshore-onshore model, *Marine Geology* 268, p 43-54, 2010

Ramaswamy, V., Rao, P.S., Grain size analysis of sediments from the northern Andaman Sea: Comparison of laser diffraction and sieve-pipette techniques. *Journal of Coastal Research* 22:1000-1009, 2006

Reading, H., *Sedimentary environments: processes, facies and stratigraphy*, Blackwell, London, 1996

Regnaud H., Cocaign J-Y., Saliège J-F., Fournier J., In situ building of dunes since the Sub Boreal (3600 BP): evidence of chronological continuity on the northern coast of Brittany. An example in Anse du Verger (Ille-et-Vilaine), *Comptes Rendus de l'Académie des Sciences* 321, p 303-310, 1995

Reineck, H.E., Singh, I.B., *Depositional sedimentary environments*, Springer-Verlag, Berlin, 1980

Rivière, A., *Méthodes granulométriques. Techniques et interprétation*, Gulf Publishing Company, Houston, 1932

Rivière, A., Vernhet, S., Contribution à l'étude de la sédimentation des sédiments carbonatés, reprinted from *Developments in Sedimentology*, Vol. 1, L. M. J. U. van Straaten (Editor), *Deltaic and Shallow Marine Deposits*, Elsevier Publishing Company, Amsterdam, 1964

Rodriguez, J.G., Uriarte, A., Laser diffraction and dry-sieving grain size analyses undertaken on fine- and medium-grained sandy marine sediments: a note. *Journal of Coastal Research* 25: 257-264, 2009

Sneed, E.D., Folk, R.L., Pebbles in the Lower Colorado River, Texas: a study in particle morphogenesis. *Journal of Geology* 66: 114-150, 1958

Tessier B., Poirier C., Weill P., Dezileau L., Rieux A., Mouazé D., Fournier J., Bonnot-Courtois C., Evolution of a shelly beach ridge system over the last decades in a hypertidal open-coast embayment (western Mont-Saint-Michel Bay, NW France), *Journal of Coastal Research* SI(88), p 77-88, 2019

Trask, P.D., *Origin and Environment of source sediments of petroleum*, Masson, Paris, 1977

Tucker, M.E., *Sedimentary petrology*, Blackwell, London, 2001

Udden, J.A., Mechanical composition of clastic sediments. *Bulletin of the Geological Society of America* 25: 655-744, 1914

Vaslet, D., Larsonneur, C., Auffret, J.P., *Carte des sédiments meubles superficiels de la Manche à 1/500,000*, BRGM-IFREMER, carte géologique de la marge continentale, Orléans, 1979

Vatan, A., *Manuel de sédimentologie*, Technip, Paris, 2000

Verger, F., *Marais et wadden du littoral français, étude de géomorphologie*, Thèse, Bordeaux, 1968

Wentworth, K.H., A scale of grade and class terms for clastic sediments. *Journal of Geology* 30: 377-392, 1922

Zingg, T., Beitrag zur schotteranalyse. *Schweiz. Mineral. Petrogr. Mitt.* 15: 39-140, 1935

Table of Contents

Chapter 1 Definitions	6	5.1 Grain Shape	40
1.1 Dry and Wet Sieving Principle	6	5.1.1 Sphericity	40
1.2 Sedimentometry Principle	6	5.1.2 Flattening and Bluntness	40
1.3 Laser Diffraction Granulometry Principle	7	5.1.3 Lengthening	40
1.4 Image Analysis	7	5.1.4 Roundness	40
1.4.1 Grain morphoscopy	7	5.1.5 Miscellaneous	41
1.4.2 Quartz exoscopy	7	5.2 Calcimetry	44
1.5 Granulometric Definitions and Size Classes	9	5.2.1 Sample preparation	44
		5.2.2 Operating mode	45
		5.2.3 Calculation of $CaCO_3$ content	47
		5.3 Organic Matter	47
		5.3.1 Operating mode	47
		5.3.2 Calculation of OM content	47
		5.4 Water Content	47
		5.4.1 Dosage	48
		5.4.2 Concentration calculation for wet sediment	48
Chapter 2 Field Sampling	12	5.5 Settling and Rheology of Silts	48
2.1 Particle Size Analysis	12	5.5.1 Granulometric, mineralogical and chemical characteristics of muddy sediments	48
2.1.1 Indirect Access to Field	12	5.5.2 Falling speed and particle flocculation	49
2.1.2 Direct Access to Field	12	5.5.3 Silt settling	50
2.2 Stratigraphic Analysis	13	5.5.4 Physical properties of a solid particle in stille water	51
2.2.1 Hand held Corer	14	5.5.5 Set of particles	51
2.2.2 Reineck Box Core	14		
2.2.3 Tube and Multi-tube Corers	14		
Chapter 3 Sieving Equipment	16	Chapter 6 Sediment Mapping	54
3.1 Sampling and Storage	16	6.1 Map Legend	54
3.2 Washing and cleaning	17	6.2 Seabed Types	56
3.3 Drying	18	6.3 Sedimentary Facies	56
3.4 Separating	18	6.4 Operating Mode	57
3.5 Sieving	19		
3.6 Weighing	19	Chapter 7 Sedimentological Maps	58
3.7 Carbonizing	20	Personal notes	66
3.8 Calcium Carbonate	20	Bibliography	68
		Table of contents	73
Chapter 4 Grain Size Analysis	22		
4.1 Sample Treatment	22		
4.1.1 Choice of sediment fraction to be considered	22		
4.1.2 Coarse fraction	22		
4.1.3 Fine fraction ($< 20 \mu m$)	23		
4.1.4 Granulometric analysis diagram	23		
4.1.5 Granulometric techniques	28		
4.2 Data Processing	29		
4.2.1 Percentile method	29		
4.2.2 Position parameters	29		
4.2.3 Dispersion parameters	29		
4.2.4 Assymmetry parameters	32		
4.2.5 Sharpness parameters	33		
4.3 Graphical Representation	33		
4.3.1 Evolution index method	34		
4.4 Granulometric Index Method	37		
4.5 Image Processing	38		
Chapter 5 Other Conventional Analyses	40		

This practical guide is designed for students conducting granulometric analyses of sediments collected in the field, whether on foot or aboard oceanographic vessels. It covers essential definitions and explores various technical approaches for sediment analysis. The guide begins with an overview of the primary sampling methods, followed by a detailed presentation of the laboratory equipment. It then delves into the granulometric analyses themselves, explaining the fundamental formulas for granulometric statistics. Additionally, it discusses methods for studying grain shape, measuring carbonate content, organic matter, and water content. The guide concludes with examples of sediment mapping.



Jérôme Fournier-Sowinski is a researcher at the CNRS. He has worked at several marine stations run by the Ecole Pratique des Hautes Etudes and the Muséum National d'Histoire Naturelle in Dinard and Concarneau. Part of his work focuses on coastal geomorphology and sedimentology.

Cover: Honeycomb worm reef, Mont Saint-Michel Bay, France



IX, 2024



STATION MARINE
CONCARNEAU